The development of immunological tools as methods to investigate T cell dynamics.

By:

Omar Jawaid
B.S. Loyola University Chicago, 2005

THESIS

Submitted as partial fulfillment of the requirements
for the degree of Masters of Science in Microbiology/Immunology
in the Graduate College at the
University of Illinois at Chicago, 2012

Chicago, Illinois

Defense Committee:

Zheng Chen, Chair and Advisor
Nancy Freitag
Alan McLachlan

TABLE OF CONTENTS

LIST OF FIGURES

LIST OF ABBREVIATIONS

MHC	Major Histocompatability Complex
TCR	T-cell Receptor
SEB	Staphylococcus Enterotoxin B
TSST-1	Toxic Shock Syndrome Toxin-1
IM	Intramuscular
HMBPP	(E)-4-hydroxy-3-methyl-but-2-enyl pyrophosphate
HIV	Human Immunodeficiency Virus
IMAC	immobilized metal affinity chromatography
PBS	Phosphate Buffered Saline
BCA	Bicinchoninic Acid
PBMC	Peripheral Blood Mononuclear Cells
CFSE	Carboxyfluorescein Succinimidyl Ester
R10	RPMI-1640 + 10% Fetal Bovine Serum
FBS	Fetal Bovine Serum
MOI	Multiplicity of Infection
PVDF	Polyvinylidene Fluoride
HRP	Horseradish Peroxidase
FPBS	Phosphate Buffered Saline + 10% FBS
MTE	*Mycobacterium tuberculosis* extracts

SUMMARY

The development of new immunological tools is necessary in order to answer outstanding questions in immunology. Prior evidence has been put forth regarding a superantigen in *Mycobacterium tuberculosis*, however, attempts to isolate this hypothesized agent have been unsuccessful. The use of MHC-II tetramers to identify the hypothesized superantigen has been theorized; attempts to construct this immunological tool have been unsuccessful. Here, a detailed methodology to purify, construct and use MHC-II tetramers is provided. DR*201, an MHC-II allele, was previously subcloned into *Drosophila melanogaster* embryonic cells with the following modifications: removal of the transmembrane domain, addition of an N-terminus secretion signal, C-terminus 6xHisTag, an N-terminus biotinylation signal and the antigenic peptide Ag85 linked via a flexible glycine region. DR*201 was purified on the basis of 6xHisTag binding to cobalt cations as well as binding to avidin by means of biotin and tetramerized via streptavidin binding to four biotinylated molecules of DR*201. DR*201 tetramers were then used in PBMC cell culture to assess whether or not the DR*201 tetramer or DR*201 tetramer complexed with superantigen could induce the proliferation of T cells. It was hypothesized that DR*201 complexed with superantigen would induce proliferation of T cells, while DR*201 tetramer alone would be insufficient to proliferate T cells. DR*201 tetramers were found to not proliferate T cells, as expected, however, it was found that DR*201 complexed with superantigen blocked T cell proliferation, contrary to the hypothesis. This raised the possibility that additional signals were needed to induce T cell proliferation. A further

investigation into this observation is warranted in order to understand the full repertoire needed to expand T cells in culture.

In addition, a *Listeria monocytogenes* expression vector was constructed such that *Macaca mulatta* IL-22 protein was expressed via a mutant strain under the control of constitutively active virulence associated PrfA transcription factor, designated PrfA*. This allows the protein under the control of PrfA to be expressed to high levels. Upon infection, *Listeria monocytogenes* exists as an intracellular pathogen, which allows for the intracellular delivery of expressed proteins. Prior research has implicated IL-22 in Vγ2Vδ2 T cell kinetics. Depending on the context of investigation, IL-22 is able to induce or prevent Vγ2Vδ2 T cell expansion. *Listeria monocytogenes* expression of intracellular IL-22 was used to deliver IL-22 to THP-1 macrophages *in vitro* and the ability of these infected macrophages to expand Vγ2Vδ2 T cells was assessed. It was hypothesized that PBMCs co-cultured with THP-1 macrophages infected with IL-22 expressing *L. monocytogenes* would induce the expansion of Vγ2Vδ2 T cells. These PBMCs were assessed for Vγ2Vδ2 T cell proliferation and no significant proliferation was detected in these experiments. However, a significant bias towards CD3+ lymphocytes was observed when THP-1 macrophages were infected with PrfA* *Listeria monocytogenes*, but not wild-type *Listeria monocytogenes*, and warrants further investigation as to the composition and kinetics of the observed expansion of CD3+ lymphocytes.

I. Introduction

A. **Background information.**

Studying the immune system requires varied, robust tools in order to answer profound questions with sufficient power. Developing these tools is a key focus of interest in laboratories around the world, including our own laboratory. In these studies, we demonstrate the construction and use of two such tools. One tool which has seen more recent use is the MHC-II tetramer. Originally, tetramers were constructed using soluble, biotinylated MHC-I molecules consisting of α and β_2 microglobulin subunits, on a streptavidin backbone, resulting in 4 MHC-I molecules bound to streptavidin (Wooldridge *et. al.*, 2009). This entire construct was called an MHC-I tetramer. Use of this construct allowed for long-lived interactions between CD8+ T lymphocytes and antigen-specific MHC-I tetramers. Previously, these types of interaction were difficult to study because the MHC-I:T cell receptor (TCR) interaction is extremely short-lived, on the order of seconds. With tetramer technology, multiple MHC-I molecules can bind to multiple TCR molecules on the T cell of interest, generating a long-lived interaction that remains stable for hours or days (Wooldridge, *et. al.* 2009). With this increased binding strength, analysis by flow cytometry became possible. By combining fluorescent dyes with tetramer technology, antigen-specific CD8+ T cells could be studied in detail for the first time.

Similar to MHC-I tetramers, MHC-II tetramers have been constructed to study CD4+ antigen-specific T cells. However, several challenges present when dealing with the MHC-II molecule Because peptide loading and MHC-II folding are intricately intertwined, it is much more difficult to

construct stable MHC-II molecules that can be used in the tetramerization process (Villadangos *et. al.*, 2005). This is in stark contrast to MHC-I molecules, which can fold properly in the absence of peptide. Furthermore, even when stable MHC-II molecules can be obtained, the MHC-II TCR interaction is an order of magnitude or more weaker than the MHC-I TCR interaction (Cole *et. al.* 2007). One mechanism to avoid the instability of MHC-II folding and peptide loading is to covalently link the peptide of interest to the C-terminus of the MHC-II molecule with a flexible glycine linker (Wooldridge *et. al.* 2009). This method allows for correct folding of the MHC-II molecule with a peptide loaded into the peptide binding groove; this comes at the expense of versatility as each peptide-MHC-II molecule would have to be individually constructed. However, these drawbacks still have not deterred researchers from using MHC-II tetramers to study CD4+ antigen-specific T cell populations. Our laboratory has used these MHC-II tetramers to investigate CD4+ T cells in the periphery and in infected tissue in a macaque model of *Mycobacterium tuberculosis* infection (Wei *et. al.* 2009). Here, it was found that a population of Ag85 antigen-specific CD4+ T cells could be detected in the lymph, spleen and lung tissues of infected macaques. In addition to detecting these lymphocytes, we also demonstrated the kinetics of proliferation differed significantly in these infected tissues as compared to the periphery. Previous researchers could not find such a population in *M. tuberculosis* infected BALB/c mice and this finding represented a significant breakthrough in the investigation of CD4+ T cells in *M. tuberculosis* infected tissues.

One active area of research is the use of MHC-II:TCR interactions to study superantigens. Superantigens crosslink MHC-II molecules to the TCR by binding to conserved regions; this allows for tight, indiscriminate binding to T cells (Novick 2003). This non-specific crosslinking of the TCR to

MHC-II can cause large numbers of T cells to become activated and proliferate profusely which can lead to massive inflammation, fever, rashes and more seriously, shock, organ failure and death (Novick 2003). Superantigens are an important virulence factor involved in bacterial and viral infections. Classically, *Staphylococcal aureus*, *Streptococcus pneumoniae,* and *Streptococcus pyogenes* secrete superantigens during the course of infection (Llewelyn, *et. al.* 2002). These proteins bind to conserved regions, either on the α or β chains of the MHC-II molecule, and crosslink the MHC-II molecule to the TCR, again by binding to conserved regions on the α or β chain on the TCR. Traditionally, superantigens have been identified by their ability to cause activation and/or proliferation of T cells in a non-specific manner. In some cases, a specific subset of Vβ T cells are activated such that these T cells are overrepresented in tissues or tissue culture; this also fits the definition of a superantigen (Watanabe-Ohnishi *et. al.* 1995).

M. tuberculosis is a causative agent of pulmonary tuberculosis and infects over 9 million people per year (WHO 2009). *M. tuberculosis* pathogenesis is characterized by a long incubation time in which the bacterium colonizes the alveoli, lung macrophages and possibly the lymphatic system. When confined to the lungs, the bacteria slowly form fibrous, impregnable granulomas. These granulomas harbor latent bacteria which can subsequently reactivate upon some stressor and lead to inflammation and tissue destruction (WHO 2009). *M. tuberculosis* is often characterized solely as a pulmonary pathogen; however, *M. tuberculosis* can also infect other parts of the body, such as spleen, liver, the abdomen, the central nervous system and the brain. Although antibiotic treatments can be successful in clearing the bacteria from the lungs, the rise of multidrug resistant strains is an increasing cause for concern. Because *M. tuberculosis* is able to colonize and survive in multiple niches in the

human body, an understanding of the set of virulence factors involved in pathogenesis is a crucial focus of research. *M. tuberculosis* produces a wide variety of virulence factors, implicating in immune suppression, survival in macrophages, inhibition of inflammatory cytokine production, and granuloma production (Reed *et. al.* 2004, Chan *et. al.* 1991, Nigou *et. al.* 2001, Manganelli *et. al.* 2001, Smith 2003). Although *M. tuberculosis* is generally thought not to produce a superantigen, several hallmarks of a superantigen molecule can be detected (Ohman *et. al.* 1994). When patients with confirmed *Mycobacterium tuberculosis* infections were examined, several hallmark signs of a superantigen were detected. The researchers determined that the Vβ8 TCR was overrepresented in these infected individuals. Furthermore, the kinetics of whole *M. tuberculosis* extracts (MTE) instigated a T cell proliferation profile resembling staphylococcal enterotoxin E (SEE). Finally, MTE could induce CD4+ and CD8+ T cells to proliferate non-specifically, and crucially, this proliferation could be blocked with the addition of anti-HLA-DR antibody, suggesting that MHC-II involvement is necessary for the proliferation of T cells. This is a hallmark of superantigens. However, despite this evidence, no such protein or factor has been identified.

We hypothesize that the use of MHC-II tetramer technology may be able to identify the agent in *M. tuberculosis* that is responsible for the observed superantigen effects on T cells. Since superantigens bind tightly to MHC-II, we hypothesize that using MHC-II tetramers will selectively purify any superantigen or superantigen-like molecules from MTEs and induce proliferation of T cells in PBMC cell culture. Supposing that this is the case, the MHC-II tetramer can then be used to purify and isolate the molecule of interest and allow us to study the molecule responsible in detail. The first key step is to develop a reliable and robust protocol to construct MHC-II tetramers and then develop the T cell

expansion assay. The development of these tools allows us to address a number of questions related to the superantigen mechanism of action as well as investigating questions of antigen presentation, CD4+ T cell kinetics, the localization of CD4+ T cells during infection, characterization of alloreactive T cells, and determining the specific outcomes of CD4+ and CD8+ activation.

IL-22 is a cytokine involved in the initial inflammatory response as well as the secondary inflammatory response (Pestka *et. al.* 2004). In response to IL-22 secretion by innate lymphoid cells, epithelial-derived cells are able to produce anti-microbial and anti-fungal peptides and allow leukocytes and natural killer cells to infiltrate tissues (Sanos *et. al.*, 2010). Furthermore, IFN- γ producing γδ T cells downregulate the secretion of IL-22. Simultaneously, IL-22 can induce the proliferation of γδ T cells (Yao *et. al.* 2008). Moreover, IL-22 producing T cells, Th17 helper T cells, have been implicated in autoimmunity and dysregulation of IL-22 has been implicated in these conditions (Dubin *et. al.* 2008). One of the initial lines of defense is the mucosal lining. Pathogens, such as *Listeria monocytogenes*, *Salmonella enterica, Mycobacterium tuberculosis*, Herpes simplex virus, HIV-1, several *Shigella* species and *Escherichia coli* all invade via the mucosal lining of the gastrointestinal tract or the respiratory tract (Xavier *et. al.* 2007, Eckburg *et. al.* 2005, Butcher *et. al.* 1999). Identifying the key components of mucosal immunity, such as IL-22, allows for the development of more selective, more effective vaccines. It has been long known that vaccines administered mucosally are more effective than intramuscular (IM) or subcutaneous vaccines (Neutra, *et. al.* 2006). However, the components of engineering an effective mucosal vaccine remain elusive. As of yet, no defining characteristic has been identified which leads to strong mucosal immunity. IL-22 is one component, of many, which has been shown to aid in mucosal immunity. In a candidiasis infection, in which mice

were topically infected with *Candida albicans*, IL-22 was able to activate epithelial cells to produce anti-fungal and anti-bacterial peptides. In addition, IL-22 production was linked to preventing other secondary infections by *Saccharomyces cerevisiae* and *Cryptococcus neoformans (*De Luca, *et. al.* 2010). IL-22 has also been shown to be produced by γδ T cells as well as be regulated by these cells. γδ T cells are involved in a variety of roles, involving both innate and adaptive immunity. Although they only compromise a small percentage of the T cell population, they play an important role in coordinating the adaptive immune response by producing IFN-γ and acting as professional antigen presenting cells (Petska, *et al* 2004, Kaufmann 1993, Brandes *et. al.,* 2005). Moreover, γδ T cells are capable of recognizing bacterially infected cells and secreting cytotoxic agents against these cells (Qin *et. al.* 2009). In a model of chronic *M. tuberculosis* infection in macaque monkeys, our laboratory has found that γδ T cells are able to proliferate to relatively large numbers, produce IFN-γ, and suppress IL-22 production by both the innate immune system and the adaptive immune system (Yao *et. al.* 2010). Furthermore, our laboratory has shown that the addition of phosphoantigens, such as the bacterially-derived phosphoantigen (E)-4-hydroxy-3-methyl-but-2-enyl pyrophosphate (HMBPP), can induce Vγ2Vδ2 expansion. Phosphoantigens are intermediate metabolites which are necessary for biosynthesis of key molecules in all living organisms. Significantly, the immune system can recognize these intermediate metabolites produced by bacteria such as *Listeria monocytogenes* and *Mycobacterium tuberculosis*; these phosphoantigens may serve as another signal for immune cells to proliferate and attack sites of infection (Wei *et. al.* 2009). By studying the kinetics, activity and distribution of Vγ2Vδ2 T cells, significant insight into immunological crosstalk can be gleaned.

We hypothesize that the use of *Listeria*-based delivery systems can allows the investigation of the role of IL-22 in bacterial infection. By using a *Listeria*-based vaccine vector, we can assess the role of IL-22 as an adjuvant while immunizing individuals against *Listeria* expressed antigens. *Listeria*-based vaccine vectors have been postulated to be an attractive means to delivery antigens to the immune system because virulence can easily be attenuated and *L. monocytogenes* naturally infects the mucosal membranes during its lifecycle. These traits may result in an effective vaccine against pathogens that invade the mucosal lining such as HIV, tuberculosis, enterohemorrhagic *Escherichia coli*, and other such pathogens (Starks, *et. al.* 2004). Previously, we have shown that the use of *Listeria* vaccine vectors results in strong humoral and cellular immunity against tuberculosis derived antigens (Yan, *et. al.* 2008). One of the key features of this system is the use of the NF-972 and NF-974 strains, deemed prfA*. These mutants can express genes under the control of a prfA promoter to a very high level. This is due to the fact that the PrfA transcription factor has been rendered constitutively active by key point mutations. Normally, PrfA is only activated during the course of infection and is responsible for the production of gene products involved in pathogenesis (Renzoni *et. al.*, 1997). When an exogenous gene is placed under the control of a promoter activated by PrfA, large amounts of that gene product can be detected. Using the hly promoter, which is under the control of PrfA, allows us to exploit *Listeria*'s own secretion machinery to secrete selected proteins into the extracellular environment. In addition to being prfA* mutants, these strains are also attenuated in infection by virtue of the ΔactA mutation. ActA is responsible for the cell-to-cell spread of *Listeria* and without this gene, infection is attenuated by up to 1000-fold (Yan *et. al.,* 2008). By subcloning the IL-22 gene into these *L. monocytogenes* strains and assessing the impact that this cytokine has on infected cells in PBMC

culture, we can ascertain whether or not IL-22 is an appropriate addition to the *L. monocytogenes* vaccine vector. Furthermore, we can investigate the kinetics of IL-22 with respect to T cell proliferation as well as investigating the feedback cycles in IL-22 production. These questions remain outstanding in the field of cytokine immunology and the development of this tool will allow us to probe the answers to these questions.

II. Materials and Methods

A. S2 cell culture and DR*201 protein expression.

S2 *Drosophila melanogaster* embryonic cells were cultured in 175 cm^2 tissues culture flasks (BDBiosciences) with filtered Schneider's complete *Drosophila* medium (1x, Invitrogen). Complete media is defined as Schneider's media containing 20mM glutamine (Gibco) and 10 μg/mL blastocidin (Sigma Aldrich). S2 cells were maintained at a cell density of 2 x 10^6 to 1 x 10^7 cells/mL in 40 mL of Schneider's complete media and cultured at room temperature. After 3-4 days of growth, S2 cells were passaged 2:1 in fresh media and assessed for cell viability by trypan blue exclusion. Typically, cell viability was >95%. This process was repeated until 8-12 flasks of S2 cells were obtained. These flasks were then induced to secrete soluble DR*201.

DR*201 expression was designed to be controlled by the metallothionein promoter. DR*201 is composed of a 33 kDa α chain and a 28 kDa β chain (Wei *et. al.* 2009). The transmembrane domain of DR*201 was removed to facilitate solubility and a secretion signal, via the pCoBlast plasmid, was added to the N-terminus of the DR*201 subcloned gene. In addition, DR*201 was also modified to include a C-terminus 6xHisTag and a biotinylation signal located downstream of the secretion signal on the N-terminus. Finally, to facilitate proper folding of DR*201, a flexible glycine linker was used to link the antigenic peptide Ag85 to DR*201. This results in the binding of Ag85 to DR*201 during protein folding and maturation (Wei *et. al.* 2009). To induce DR*201 expression, cell cultures of S2 cells ready to be induced had 25mL of additional complete Schneider's media added and cultured for an additional 4 days. Copper (II) sulfate ($CuSO_4$) was then added to a final concentration of 200 μM and

cultured for an additional 3-4 days. Once induction was complete, the cell cultures were centrifuged in a table top centrifuge in 50 mL conical flasks to pellet cells and cellular debris. The supernatant was collected and filter-sterilized using a 0.22 μM vacuum filter sterilizer (Millipore). This supernatant was then used in downstream experiments to isolate the DR*201 protein.

B. **Immobilized metal ion chromatography (IMAC) purification of DR*201.**

First stage purification of DR*201 was accomplished through immobilized metal affinity chromatography (IMAC). DR*201 contains an N-terminus 6xHisTag, allowing for tight binding with cobalt cations. In order to proceed with IMAC purification, filter-sterilized supernatant obtained from induced-S2 cells were concentrated in a 15mL, 30 kDa centrifugal filter unit (Millipore). The retained supernatant with an approximate volume of 250 μL was then collected, filter-sterilized and dialyzed 400:1 against 1x phosphate buffered saline (PBS) using 3 kDa SnakeSkin dialysis tubing (Pierce Scientific). After 3-5 hours, the original PBS was discarded and fresh PBS was added to continue dialysis overnight at 4 ºC. The next morning, 500 μL of HisPur Cobalt agarose resin (Pierce) was placed into a gravity flow column, washed with Wash/Equilibrium solution (50 mM sodium phosphate, 300 mM sodium chloride, 10 mM imidazole; pH 7.4) and the solution was drained. DR*201 containing supernatant was then incubated with HisPur resin, capped and mixed on a table top rotor for 15-60 minutes. The resulting solution was then collected, labeled as cobalt-treated supernatant, filter-sterilized, and stored at 4 ºC. The resin, now bound with DR*201, was washed with 5 supernatant volumes of Wash/Equilibrium solution. These washes were collected, filter-sterilized and stored at 4 ºC. To elute DR*201, 10 mL of Elution solution (50 mM sodium phosphate, 300 mM sodium chloride,

150 mM imidazole; pH 7.4) was added to the HisPur resin and incubated for 30 minutes. The solution was then drained, filter-sterilized and dialyzed 400:1 against 10 mM Tris-HCl pH 8.0 (Sigma Aldrich) for several hours. After 3-5 hours, the original buffer was discarded and fresh Tris-HCl, pH 8.0 was added to continue dialysis overnight at 4 ºC. It was decided that the cobalt-treated supernatant and subsequent washes did not warrant dialysis treatment as the eluted DR*201 protein.

C. **Biotinylation of DR*201 via BirA ligase.**

When subcloned into the S2 expression vehicle, the DR*201 gene was modified to include a C-terminus AviTag (GLNDIFEAQKIEWHE, Avidity). *Escherichia coli* biotin ligase (BirA) is highly specific and sensitive to this sequence, attaching a molecule of biotin to lysine within the AviTag sequence (Schatz *et. al.*, 1993). DR*201 cobalt eluate was removed from dialysis tubing and concentrated in a 15 mL, 30 kDa centrifugal filter unit (Millipore). The retained solution was then biotinylated according to the following reaction conditions: 100 µL supernatant, 13 µL Biomix A, 13 µL Biomix B and 4 µL BirA biotin ligase. A minute quantity of NaN_3, typically one or two grains of salt, was added as a preservative. The reaction was then incubated at 30 ºC overnight. Once the reaction was completed, the reaction mixture was placed into 10mL of 1xPBS and then dialyzed 400:1 against 1x PBS for 3-5 hours. Then, the original PBS solution was discarded, fresh 1x PBS was added and dialysis continued overnight at 4 ºC.

D. **Avidin purification of DR*201.**

Second stage purification of DR*201 was conducted using biotin selection via immobilized avidin chromatography. Avidin binds biotin with strong affinity, allowing for selective binding of biotin containing molecules. To purify DR*201, the monomeric immobilized avidin column (Pierce)

was used to select for DR*201-biotin molecules. The use of monomeric avidin allows for competitive release of DR*201-biotin by the addition of excess free biotin. The column was prepared by washing the column with 8 mL of filter-sterilized PBS. Then, 6mL of Biotin Binding and Elution solution was added to the column in order to block all non-reversible biotin binding sites. The addition of 12mL Regeneration Buffer removes biotin from the biotin-binding sites on avidin, allowing for selection of biotin containing molecules. After addition of 8 mL of PBS, the column is ready to be used. DR*201 supernatant was concentrated in 15 mL, 30 kDa centrifugal filter units and the retained solution, with an approximate volume of 250 µL, was added to PBS to a final volume of 1.75 mL. This solution was then applied to the avidin column and incubated for 60 minutes. Where appropriate, 1mL of a 5 mg/mL solution of superantigen, either toxic shock syndrome toxin 1 (TSST-1) or staphylcoccal enterotoxin B (SEB), (Invitrogen, Sigma Aldrich) was added to the column and then incubated for an additional 30 minutes. The column was then washed 6 times with 5 mL PBS. These washes were collected separately for analysis. To elute DR*201 from the avidin column, 10 mL of Biotin Blocking and Elution buffer was added to the column in 2mL increments. On the final 2 mL increment, the column was incubated for 30 minutes and then collected. The eluate was pooled together and then dialyzed 400:1 against 1x PBS for 3-5 hours. The old PBS solution was then discarded, fresh 1x PBS was added and dialysis continued overnight at 4 ºC.

E. **Dot blot detection of DR*201.**

The mouse monoclonal antibody, L243 (BDBiosciences), only detects MHC-II in the native conformation. As a result, SDS-PAGE analysis is not compatible with the detection of MHC-II using this antibody. However, other antibodies can detect denatured MHC-II protein, but were not employed

in this study (Kostelny, *et. al.* 2001). To assess DR*201, dot blots were used as protein conformation will be retained throughout the detection process. If necessary, TSST-1 bound to DR*201 was detected through a sheep polyclonal TSST-1 antibody (Abcam) and detected via goat anti-sheep HRP conjugate (Invitrogen); the rest of the protocol was unchanged. 15 μL of each sample to be analyzed was placed onto methanol-activated polyvinylidene fluoride (PVDF) membrane (Millipore) and air dried completely. SuperBlock (Sigma Aldrich) or 10% bovine serum albumin (BSA) (Sigma Aldrich) was used as the blocking reagent. Blocking proceeded by incubation at room temperature for 1 hour, and if necessary, overnight at 4 ºC. After blocking was completed, the membrane was rinsed in PBS-Tween20 (0.05% v/v). 10 μL of primary antibody was placed into 10 mL of SuperBlock or 10% BSA and incubated on the membrane at room temperature for 1 hour. The membrane was then washed 4 times in PBS-Tween20, 15 minutes per wash. 2 μL of goat anti-mouse HRP conjugated antibody (Invitrogen) was placed into 10 mL of SuperBlock or 10% BSA and incubated on the membrane at room temperature for 30 minutes. The membrane was then washed 8x in PBS-Tween20, 10 minutes per wash. To detect DR*201, 5 mL of Luminol enhancer and 5 mL Stable Peroxide Buffer (Pierce) were mixed and incubated on the membrane for 5 minutes. The membrane was then dried using absorbent filter paper and then imaged for 30 seconds and 2 minutes on X-ray film (Kodak).

F. **Tetramerization of DR*201.**

To form the soluble DR*201 tetramer, bicinchoninic acid (BCA) quantification (Sigma Aldrich) was performed to determine the concentration of DR*201 in solution. Working solution was freshly prepared by combining supplied BCA with 100 mM $CuSO_4$ at a 50:1 ratio. 2 mL of working solution was added to a 100μL dilution of DR*201 solution. After incubation at 37ºC for 30 minutes, the

absorbance was measured at 562 nm. The concentration was compared against a standard curve prepared using serial 2-fold dilutions of supplied 1 mg/mL BSA, which was prepared at the same time. After the concentration was determined in milligrams per milliliter, the molar concentration was calculated using a molecular weight of 61,000 Daltons for DR*201. This allowed for the proper molar ratio of 1:4, streptavidin to DR*201, to be used to construct the tetramer. The necessary molar concentration of streptavidin was calculated by using a molecular weight of 52,800 Daltons for streptavidin (Hendrickson, 1989**)**. After the proper amount of streptavidin was added to the DR*201 solution, the reaction proceeded overnight at 4 ºC. The next morning, the tetramer construct, with a calculated molecular weight of 296,800 Daltons, was filtered through a 250kDa centrifugal filter unit (Millipore) and both the retained solution and flowthrough solution was saved for analysis. The retained fluid was filter-sterilized twice and NaN_3 was added to a final concentration of 0.01% to act as a preservative.

G. **Peripheral blood monocyte isolation from whole monkey blood.**

Peripheral blood monocytes were isolated from whole monkey blood via Ficoll (GE Healthcare) density centrifugation. Whole blood was obtained from rhesus monkeys and then centrifuged at 2800 RPM for 12 minutes to separate blood constituents. The buffy coat was then extracted using a Pasteur pipetter and carefully overlaid over 4 mL of Ficoll. Enough R10 (RPMI-1640 + 10% fetal bovine serum (FBS), Gibco) was added to bring the volume up to 10 mL. The solution was centrifuged at 3200 RPM for 20 minutes at room temperature. The PBMC layer was then carefully extracted using a Pasteur pipetter and placed into 5 mL of red blood cell lysis solution (Sigma Aldrich). The cells were incubated for 10 minutes with periodic vortexing. Lysis was halted with the addition of 10 mL of R10

media. The mixture was then centrifuged at 2000 RPM for 10 minutes. The resulting cell pellet was then resuspended in 10 mL R10 media and centrifuged again at 2000 RPM for 10 minutes. The cell pellet was resuspended in 5 mL of R10 media, the cell number was determined and assessed for viability via trypan blue staining. Enough R10 media was then added to bring the final cell density to 2 x 10^6 cells/mL.

If necessary, carboxyfluorescein succinimidyl ester (CFSE) (Invitrogen) staining was performed. Enough CFSE, as determined by manufacturer's protocol, was added to the cell culture and incubated for 30 minutes at 37ºC. The cells were then placed on ice for 10 minutes to quench the reaction and then washed 3 times in R10 media. The cells were then re-suspended in enough R10 volume to bring the final cell density to 2 x 10^6 cells/mL.

H. **Tetramer + Superantigen *in vitro* expansion of T cells.**

Cell culture was prepared as above with CFSE stained PBMCs isolated from rhesus monkeys. 200 µL of cells were placed into 96-well round bottom plates (Sigma Aldrich). Then, approximately 4 µg of DR*201 tetramer or tetramer previously bound to superantigen was added to the cell cultures. As a positive control, a final concentration of 100 ng/mL of superantigen was added to induce T cell expansion. As a negative control, the final avidin column wash was added isovolumetrically to the PBMC cell culture. IL-2 was then added to the cell culture at a final concentration of 100 U/mL. Cells were incubated at 37ºC in 5% CO_2 for 7 days. On day 3, the cell culture was centrifuged at 2000 RPM for 10 minutes to pellet the cells and 50% of the media was removed. An equal amount of fresh media was replaced and IL-2 was added to the cell culture again to a calculated final concentration of

100U/mL; it was assumed that half the IL-2 was removed during the removal of media. The cells were re-suspended and resumed incubation at 37ºC in 5% CO_2.

I. **Surface and intracellular staining.**

Cells were surfaced stained according to protocol (Wei *et. al.* 2009). Briefly, cells were centrifuged at 2000 RPM for 10 minutes and then re-suspended in 3mL of 10% FPBS (PBS + 10% fetal bovine serum, Gibco). The cells were centrifuged at 2000 RPM for 10 minutes. The supernatant was then discarded and the cells re-suspended in 200 µL 10% FPBS by vigorous vortexing. Then, if necessary, primary antibody was added according to manufacturer's recommendations for 15 minutes. 3 mL of 10% FPBS was added to the cells and then centrifuged at 2000 RPM for 10 minutes. The supernatant was discarded and the cells were re-suspended in 200 µL of FPBS. The secondary antibody, goat anti-mouse fluorescent conjugated antibody (Invitrogen, BD Biosciences), was added to stain the primary antibody for 15 minutes at the manufacturer's recommended concentration. 3mL of 10% FPBS was added to the cells and then centrifuged at 2000 RPM for 10 minutes. The supernatant was discarded and the cells were re-suspended in 200 µL of 10% FPBS. 2 µL, 1 µL and 5 µL of CD3-APC or CD3-PeCy7, CD4-PE and CD8-PB (BD Biosciences) antibodies were added as a cocktail to the cell suspension and stained for 30 minutes. 3 mL of 10% FPBS was added to the cells and then centrifuged at 2000 RPM for 10 minutes. The supernatant was discarded and the cells were re-suspended in 200 µL of 10% FPBS. 3 mL of 1% formalin was then added to the cells, centrifuged for 10 minutes at 2000 RPM. The supernatant was then discarded and the cells were re-suspended in 200 µL of 1% formalin.

If intracellular staining was required, Golgi Plug™ protein transport inhibitor (BD Biosciences) was added to the cells and incubated at 37ºC in 5% CO_2. Then 3mL of Cytofix/Cytoperm (BD Biosciences) was added to the cells and incubated at room temperature for 45 minutes. The cells were then centrifuged at 2000 RPM for 10 minutes and the supernatant was discarded. The cells were re-suspended in 200 µL of 10% FPBS and then washed in 3mL 10% FPBS. The cells were centrifuged at 2000 RPM for 10 minutes and the supernatant was discarded. Then, primary antibody was added at twice the manufacturer's recommended concentration and stained for 45 minutes. 5 mL of 10% FBS was added to the cells and the cells were pelleted by centrifugation at 2000 RPM for 10 minutes. After the supernatant was discarded and cells resuspended in 200 µL of 10% FPBS, secondary antibody was added at five times the manufacturer's recommended concentration and stained for 60 minutes. After addition of 5 mL of 10% FPBS, the cells were pelleted at 2000 RPM for 10 minutes, resuspended in 5 mL 1% formalin, pelleted again at 2000 RPM for 10 minutes and finally resuspended in 200 µL of 1% formalin for flow cytometry analysis.

J. **Subcloning IL-22 into *Listeria monocytogenes.***

The IL-22 gene was previously subcloned into *Lactococcus lactis* using the plasmid pXmh (Zeng, *et. al.* 2011). To subclone the IL-22 gene into *L. monocytogenes*, primers were designed to simultaneously amplify IL-22 and change the restriction sites from XbaI to BamHI to facilitate subcloning into pPL6 (Yan *et. al.* 2008). The primers (Operon) used were as follows : 5' ATG **GGA TCC** ATG GCG CCC GTC AGC TCC CAC 3', 5' ACA T**AC TAG T**AA TGC AGG CAT TTC TCA GAG 3'. The restriction sites for BamHI (5' GGATCC 3') and SpeI (5' ACTAGT 3') are bolded. To amplify the IL-22 gene, plasmid DNA from *Lactococcus lactis* was isolated using the QiaQuick

Plasmid isolation kit (Qiagen). The DNA was subsequently used as template in PCR reactions (Invitrogen) using the following program : 95 ºC for 5 minutes, 35 cycles of 94 ºC for 30 seconds, 55 ºC for 1 minute, 72 ºC for 1 minute, and a final extension at 72 ºC for 10 minutes. PCR reactions were purified using the QiaQuick DNA purification kit (Qiagen) and stored at -20 ºC. pPL6 DNA was isolated according to manufacturer's protocol from previously transformed *E. coli* using the QiaQuick Plasmid isolation kit and subsequently stored at -20 ºC.

Digests on IL-22 and pPL6 were performed sequentially with BamHI (New England Biolabs) performed first according to supplied protocol followed by DNA purification using the QiaQuick DNA purification kit. After DNA purification, SpeI digest was performed following the protocol supplied by the manufacturer (New England Biolabs). After restriction enzyme digestion was completed, the DNA was purified as before using QiaQuick DNA purification kit. Ligation reactions were performed using T4 DNA ligase (Gibco) in the following reaction : 16 µL IL-22 column-purified PCR amplicon, 1µL column-purified pPL6, 2 µL 10x T4 DNA ligase buffer, 1 µL T4 DNA ligase. The reaction proceeded for 30 minutes at room temperature. After ligation reaction was completed, the resulting ligated plasmid was directly used to transform $CaCl_2$-competent *E. coli* SM10 cells by the heat-shock method (Hanahan 1982). 2 µL of the ligation reaction was placed directly into 50 µL of thawed, competent *E. coli* cells and incubated for 10 minutes on ice. The cells were heat shocked by placing into a 42 ºC water bath for 45 seconds then immediately placed on ice for 5 minutes. The cells were then placed into 2 mL pre-warmed LB broth and incubated with shaking for 1 hour at 37ºC. After 1 hour, aliquots of the culture were plated onto 170 µg/mL LB-chloramphenicol selective plates. The plates were then incubated at 37ºC for 24-72 hours until colonies formed. Several colonies were picked and grown in

LB broth, supplemented with 170 μg/mL chloramphenicol, to make frozen glycerol stocks. These colonies were tested for the presence of the IL-22 gene through plasmid purification and PCR of the IL-22 gene.

To transform *L. monocytogenes, E. coli* SM10 cells, transformed with either pPL6-IL-22 or pPL6, were conjugated with *L. monocytogenes*. Upon pPL6 introduction into the cytoplasm of *L. monocytogenes*, the plasmid linearizes and integrates into the genome at a neutral location. To mate SM10 with *L. monocytogenes* the following protocol was used. Fresh colonies were plated prior to the day the mating was to occur. *L. monocytogenes* was grown on BHI plates while *E. coli* SM10-pPL6-IL-22 or SM10-pPL6 were grown on LB-chloramphenicol plates. The next day, fresh BHI broth was inoculated with a loopful of *L. monocytogenes* cells while fresh LB-chloramphenicol (170 μg/mL) broth was inoculated with a loopful of *E. coli.* After growth to an optical density at 600 nm of ~0.2, 50 μL of *E. coli* and 10 μL of *L. monocytogenes* were mixed and placed onto a fresh BHI plate. The cells were mated for several hours at 37ºC. After mating was complete, the resulting colonies were re-suspended in BHI broth and plated onto 15 μg/mL chloramphenicol, 200 μg/mL streptomycin BHI plates and incubated at 37ºC for 48-96 hours. This combination of antibiotics resulted in the elimination of all *E. coli* SM10 cells as well as any *L. monocytogenes* cells that failed to integrate the pPL6 plasmid. Any colonies that grew were considered presumptive *L. monocytogenes* transformants. To confirm the presence or absence of IL-22, genomic DNA from *L. monocytogenes* was isolated using Promega Wizard Genomic Isolation Kit (Promega) as per manufacturer's protocol. This DNA was used as template to amplify IL-22 using the primers previously described.

K. **Western blot detection of *Listeria monocytogenes* expressed proteins**

The *L. monocytogenes* expression vector can express and secrete proteins into the extracellular environment. To test whether or not protein production occurred, *L. monocytogenes* strains harboring the subcloned gene of interest were incubated at 37ºC in BHI-chloramphenicol at 15 µg/mL. After overnight incubation, the cells were pelleted by centrifugation at 16,000 RPM for 10 minutes in a table top centrifuge. Supernatant was collected and concentrated using a 10kDa centrifugal filter unit (Millipore). The supernatant was treated according to Laemmli's protocol in which the supernatant was incubated at 95 ºC for 10 minutes in a 1:1 mixture of Laemmli's solution to supernatant, then cooled to room temperature (Laemmli, 1970). 40 µL of the treated supernatant was loaded into a 10% SDS gel (Pierce), run at 120V for 20 minutes then 80V for 80 minutes. After the dye front had reached the edge of the gel, the gel was washed in transfer buffer (Gibco) for 10 minutes then placed onto a methanol-activated PVDF membrane using a table top electroblotter. The membrane was then blocked with SuperBlock (Sigma) or 10% BSA for 30 minutes. 2 µL of mouse anti-c-myc or mouse anti-IL22 (Invitrogen) was mixed with 10 mL of SuperBlock or 10% BSA and incubated with the membrane for 1 hour. After 4 washes, 10 minutes per wash in PBS-Tween20 (Sigma Aldrich), 2 µL of goat anti-mouse antibody was added to 10 mL of Superblock and incubated with the membrane for 30 minutes. After 4 washes, 10 minutes per wash in PBS-Tween20, the proteins of interest were detected by adding 5mL of Luminol enhancer and 5mL Stable Peroxide Buffer (Pierce) to the membrane for 5 minutes. The membrane was then dried with absorbent filter paper and imaged twice for 30 seconds and 2 minutes on X-ray film (Kodak).

L. ***L. monocytogenes* infection and Vγ2Vδ2 T cell expansion.**

To test the hypothesis that IL-22 producing *L. monocytogenes* can induce Vγ2Vδ2 T cell expansion in the context of infection, THP-1 macrophages were infected with *Listeria monocytogenes* cells at a multiplicity of infection (MOI) of 1. THP-1 macrophages cells were counted, then resuspended in R10 media such that the final concentration of THP-1 macrophages was 1 x 10^6 cells/mL. To plate 200,000 cells/well, 200 μL of cells were placed into 96 well plates. *Listeria* cells were added to the wells to infect THP-1 macrophages at an MOI of 1. The cells were incubated for 2 hours at 37ºC in 5% CO_2. After infection had taken place, gentamicin sulfate (Gibco) was added to the culture to a final concentration of 50 μg/mL. The addition of gentamicin kills extracellular *L. monocytogenes* but not intracellular *L. monocytogenes*. After the addition of gentamicin, the cells were incubated at 37ºC in 5% CO_2 for an additional 2 hours. The macrophages were then pelleted by centrifugation at 2000 RPM for 10 minutes. The cells were washed with 200 μL of fresh R10 media and viability was assessed via trypan blue staining.

To assess Vγ2Vδ2 T cell expansion, infected macrophages and Ficoll isolated *Rhesus macaque* PBMCs, at a 50:1 PBMCs to macrophages ratio, were incubated at 37ºC, with 5% CO_2. IL-2 was added to a final concentration of 100 U/mL. The cells were then incubated for 7 days. On day 3, the cells were pelleted by centrifugation at 2000 RPM for 10 minutes, 50% of the media was removed and fresh R10 media was added. An additional amount of IL-2 was added to a final concentration of 100 U/mL; it was assumed that 50% of the IL-2 was removed through the removal of media. Cells were stained for T cell makers on the surface as well as stained intracellularly for perforin as described previously.

III. Results

A. **Purification and tetramerization of DR*201.**

The use of the 6x HisTag that was added onto DR*201 during the cloning process allows for the purification of soluble DR*201 from S2 cell supernatants using Co^{2+} agarose beads. Concentrated S2 cell supernatants were subjected to Co^{2+} agarose beads and the protein of interest was isolated. Figure 1a shows the results of a typical Co2+ purification. Concentrated S2 cell supernatant, the eluate, and a 1% BSA solution were placed onto a PVDF membrane as described and probed with mouse anti-HLA-DR antibody. Sample 1 is supernatant from induced S2 cell cultures. These cells secrete DR*201, which should be detectable by anti-HLA-DR antibodies and indeed, DR*201 can be detected as evidenced by binding of anti-HLA-DR conjugated to goat anti-mouse HRP. Furthermore, a solution of 1% BSA, shown in sample 2, does not result in any signal, indicating that the antibody is specific to DR*201. Samples 3-8 show some loss of DR*201 due to the washing of the column. This loss was limited and enough protein was recovered to proceed with downstream applications. Samples 9 and 10 show that DR*201 could successfully be eluted off cobalt agarose resin as per protocol. When the cobalt eluate was analyzed on SDS-PAGE, two bands roughly corresponding to 33 kDa and 28 kDa could be observed (data not shown). These sizes agree with established MHC-II molecular weights of the α and β chains (Wooldridge *et. al.* 2009). Qualitatively, the signal for DR*201 in the eluate is significantly more intense than in the washes, as would be expected based on protein purification using 6x HisTag binding of cobalt cations.

After purification via the 6x HisTag, demonstrated in Figure 1a, DR*201's biotinylation signal was used to add a molecule of biotin as per the protocol previously described. Although biotinylation was assumed to have occurred after following the biotinylation protocol, figure 1b demonstrates that this assumption was not unfounded. In this experiment, anti-HLA-DR was used to assess whether or not DR*201 could be successfully eluted from an avidin agarose column. Sample 1 is DR*201 purified from cobalt agarose beads and shows the expected binding to anti-HLA-DR. Sample 2 is a solution of 1% BSA, which shows no binding to anti-HLA-DR, as expected. Samples 3-8 are a series of 6 washes using PBS. As can be seen, some DR*201 loss occurred as a result of these washes. However, after elution with excess biotin, sample 9 shows, qualitatively, a significant amount of DR*201 being eluted off the avidin column. Furthermore, after stripping the avidin column using 0.1 M glycine, pH 3.0, and the immediate neutralization of this solution using 1x PBS, no DR*201 could be detected. This indicates that the excess biotin was responsible for eluting the protein of interest. This lends credibility to the hypothesis that biotinylation of DR*201 was successful and that avidin purification on the basis of this biotin molecule is possible.

Furthermore, figure 1c demonstrates that the use of the avidin column could be used to complex superantigen to DR*201 during the purification procedure. Prior to washing the avidin column with PBS, a 5mg/mL solution of TSST-1 or SEB was passed through the column. This would allow the superantigen to bind to DR*201 and theoretically remain complexed with DR*201 through the remaining purification procedures. After addition of the superantigen solution, the avidin purification protocol was continued with no modifications. Figure 1c demonstrates that TSST-1 could be detected in the eluate, as would be expected if TSST-1 was complexed with DR*201. Sample 1 is a solution of

purified TSST-1 directly placed onto the membrane. After binding with sheep anti-TSST-1 antibody and conjugation with goat anti-sheep HRP antibody, a signal can be observed where the TSST-1 was placed onto the membrane. By contrast, a solution of DR*201 was not detected by anti-TSST-1, as shown in sample 2. This indicates that the antibody is specific to TSST-1 as expected. Samples 3-8 show that some TSST-1 remained unbound and was subsequently washed off during the washing procedure. As can be seen in sample 8, TSST-1 was undetectable at this point. In this purification, TSST-1 shows a paradoxical response to washing, where later washes result in even more TSST-1 being eluted from the avidin column. This observation was not replicated in other experiments, which showed that TSST-1 elution gradually being reduced by subsequent washes of PBS. Although qualitative in nature, it was assumed that this lack of a signal signified that this wash solution was effectively vacant of TSST-1 protein. Samples 9 and 10 show that after elution with excess biotin, TSST-1 was detected in the eluate. Because TSST-1 is able to bind to MHC-II molecules, it was assumed that the TSST-1 detected in the eluate was due to TSST-1 binding to DR*201 and subsequently being co-eluted with DR*201 with the addition of excess biotin.

Although this mechanism is highly plausible in explaining TSST-1's presence in the eluate, it is not the only explanation. Two experiments, which should have been conducted, were to test whether or not TSST-1 can actually bind to DR*201 as well as demonstrating that TSST-1 added to an empty avidin column does not result in TSST-1 being eluted with the addition of excess biotin. Instead, TSST-1 should be removed due to the washing of the avidin column and thus, TSST-1 is detected in the wash solution and not the solution used to elute the avidin column. This would show that TSST-1 is not binding to the avidin column in a manner that would obfuscate the results shown here. To test

whether or not TSST-1 can bind to DR*201, a pull-down assay using TSST-1 and DR*201 could be performed. Although parts of the avidin purification process resemble a pull-down assay, the necessary controls are not present which would establish an unequivocal relationship. In the absence of these experiments, it was assumed that both TSST-1 and SEB complexed with DR*201 in a manner consistent with superantigen binding to MHC-II as classically described.

To produce MHC-II tetramers, streptavidin was added such that a ratio of 1:4 streptavidin to DR*201 was attained. To isolate DR*201 tetramers from unbound DR*201 and streptavidin, constructs were filtered against a 250 kDa filter. DR*201, TSST-1, SEB, and streptavidin alone are not large enough to prevent filtration by a 250 kDa filter, however, when 3 or 4 DR*201 molecules are bound to a single molecule of streptavidin, these constructs will be retained against the 250 kDa filter. Although this does not prove that DR*201 tetramerization has taken place, an additional experiment, shown in figure 1e, shows that the mechanism is highly plausible rather than non-specific aggregation of proteins being the cause of the high molecular weight constructs being isolated. Furthermore, because anti-HLA-DR only detects DR*201 in the native conformation, it is far more likely that DR*201 is tetramerized on a streptavidin backbone than a high molecular weight aggregate being formed. Figure 1d shows that when biotinylated DR*201 and streptavidin are incubated in a 1:4 molar ratio, they are retained against a 250 kDa filter, represented by sample 3. No DR*201 was detected in the flowthrough solution, represented by sample 4. Samples 1 and 2 demonstrate that anti-HLA-DR antibody is working as intended, as they hybridize to both biotinylated DR*201 and unbiotinylated DR*201 respectively. Sample 5, a solution of 1% BSA, again shows that anti-HLA-DR antibody is specific to DR*201. Although this is not conclusive, evidence in figure 1e shows that only biotinylated

DR*201 with streptavidin or biotinylated DR*201 bound to TSST-1 and complexed with streptavidin is able to form high molecular weight constructs, indicated in samples 2 and 3. By contrast, when unbiotinylated DR*201 and streptavidin are incubated and then passed through a 250 kDa filter, DR*201 can only be detected in the flowthrough solution, evidenced in sample 4, while the solution retained against the 250 kDa filter shows no detectable DR*201. When passed through a 30 kDa filter, unbiotinylated DR*201 incubated with streptavidin is able to be detected. This experiment, although not conclusive, suggests that streptavidin is forming DR*201 tetramers by binding with biotin present on the DR*201 molecules.

Figure 1. Purification and tetramerization of DR*201.

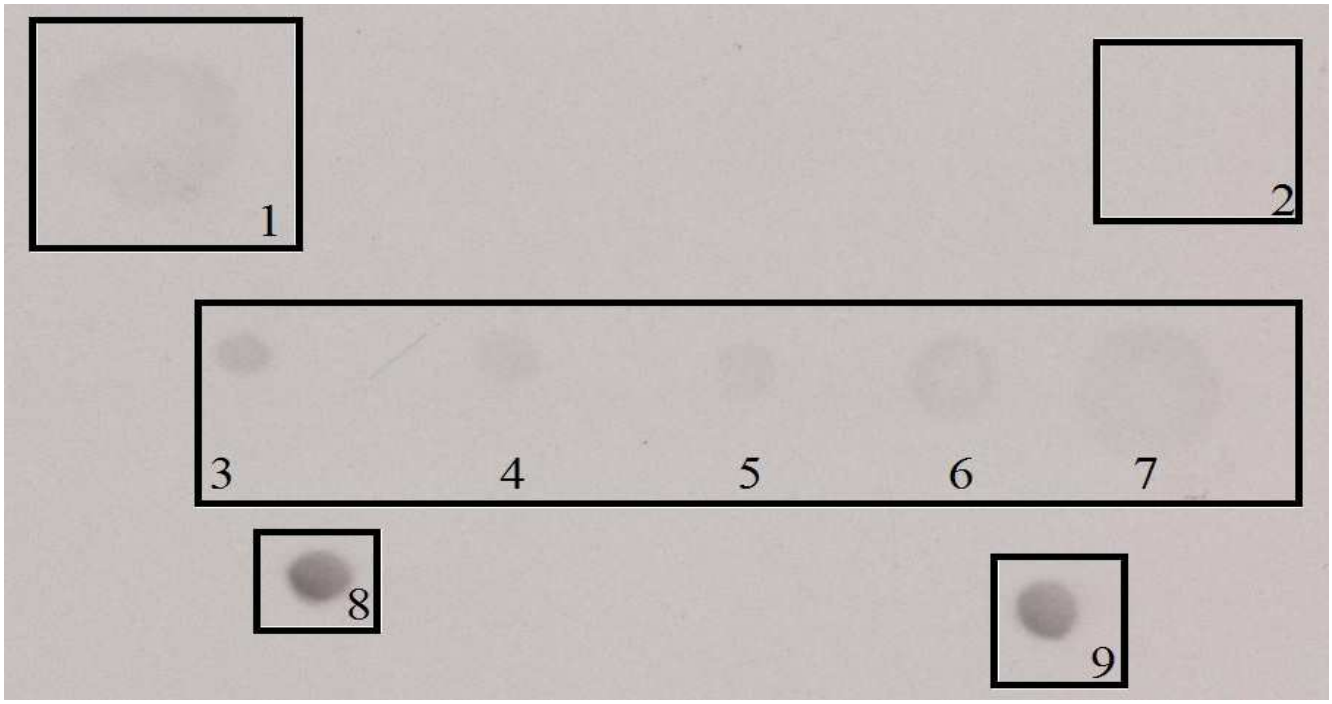

*Figure 1a. Sample 1 shows binding of DR*201 to mouse anti-HLA-DR conjugated with goat anti-mouse HRP antibody. This binding is specific to DR*201, as a solution of 1% BSA, shown in sample 2, is shown to be negative. After the Co^{2+} column was prepared and loaded as previously described, a series of 5 10mL washes was performed to remove proteins that are bound in a non-specific manner. DR*201 contains a 6x HisTag, which allows for tight binding of divalent cations, such as Co^{2+}. This tight binding should prevent DR*201 from being removed during the washing procedure. Samples 3-7 demonstrate that a small amount of DR*201 was lost during the washing procedure. DR*201 was eluted in 10mL elution buffer. Sample 8 and 9 show that DR*201 could be detected in the eluate. Although qualitative in nature, the relative intensity between the washes (samples 3-7) and the eluate show that DR*201 was purified via the 6x HisTag successfully. Since both the washes and the eluate are in similar volume size, the higher concentration of DR*201 in the eluate versus the washes can be inferred through the greater signal intensity in samples 8 and 9. Finally, when observed on an SDS-PAGE, significant bands could be observed at approximately 33 kDa and 28 kDa, representing the α and β chains of MHC-II. Thus, it was concluded that DR*201 was purified through 6x HisTag binding to Co^{2+}.*

Figure 1. Purification and tetramerization of DR*201.

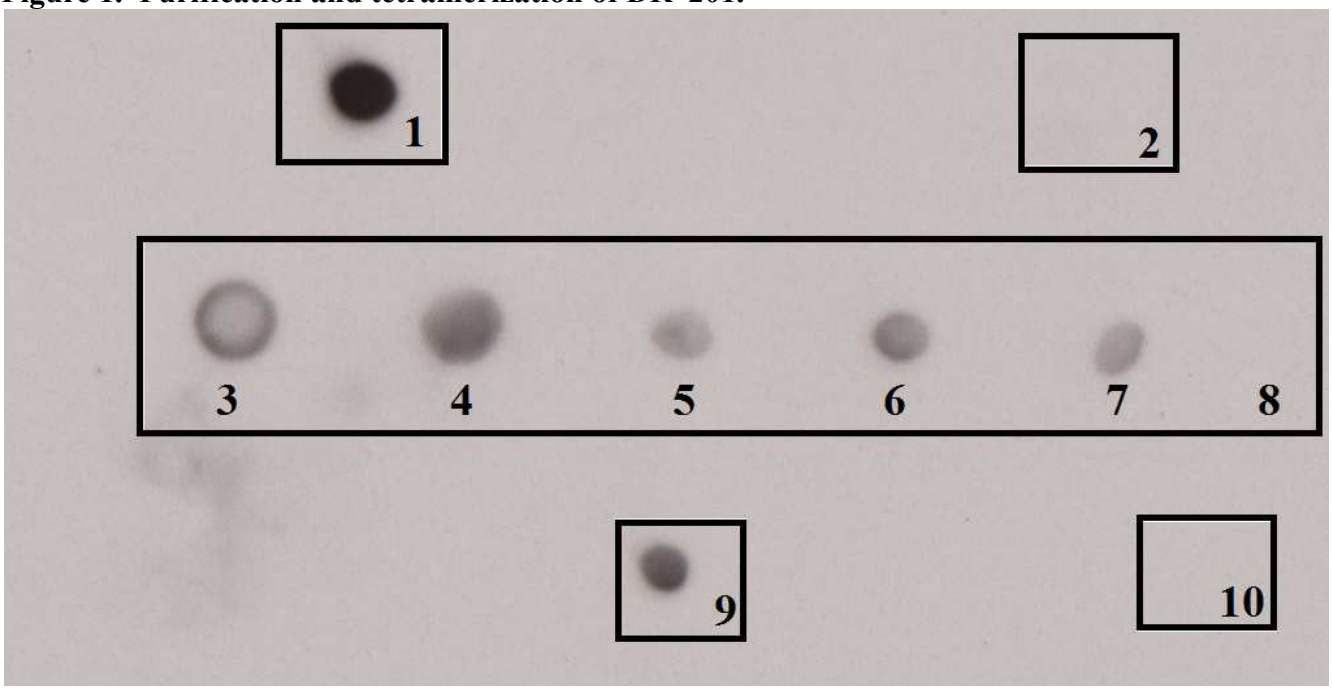

*Figure 1b. Mouse anti-HLA-DR antibody conjugated to goat anti-mouse HRP antibody was used to detect whether or not DR*201 was eluted off an avidin agarose column using biotin as the basis for purification. Sample 1 is DR*201 protein purified using cobalt agarose resin from figure 1a. As expected, anti-HLA-DR antibody hybridized successfully resulting in an unambiguous signal. A solution of 1% BSA in sample 2 shows that the antibody is specific to DR*201 indicated by the absence of a signal. After the DR*201 solution was added to the avidin column, a series of 6 washes was performed to remove proteins that bound to the column in a non-specific manner. Samples 3-8 show that these washes also co-eluted DR*201 during the washing process, although by the 6^{th} wash, DR*201 could no longer be detected. This pattern was observed regardless of the total amount of protein loaded onto the avidin column. DR*201 was eluted from the avidin column by the addition of excess biotin. The eluate, shown as sample 9, was positive for DR*201. After DR*201 was eluted, 0.1 M glycine, pH 3.0 was used to strip the avidin column. This solution was collected in 1x PBS, immediately neutralizing the solution and should theoretically preserve protein conformation. This sample was assayed for the presence of DR*201, shown as sample 10. As can be seen, no further DR*201 was detected, indicated that most, if not all, of DR*201 was eluted, although the possibility remains that the 0.1 M glycine treatment denatured DR*201 to the point which detection was not possible*

Figure 1. Purification and tetramerization of DR*201.

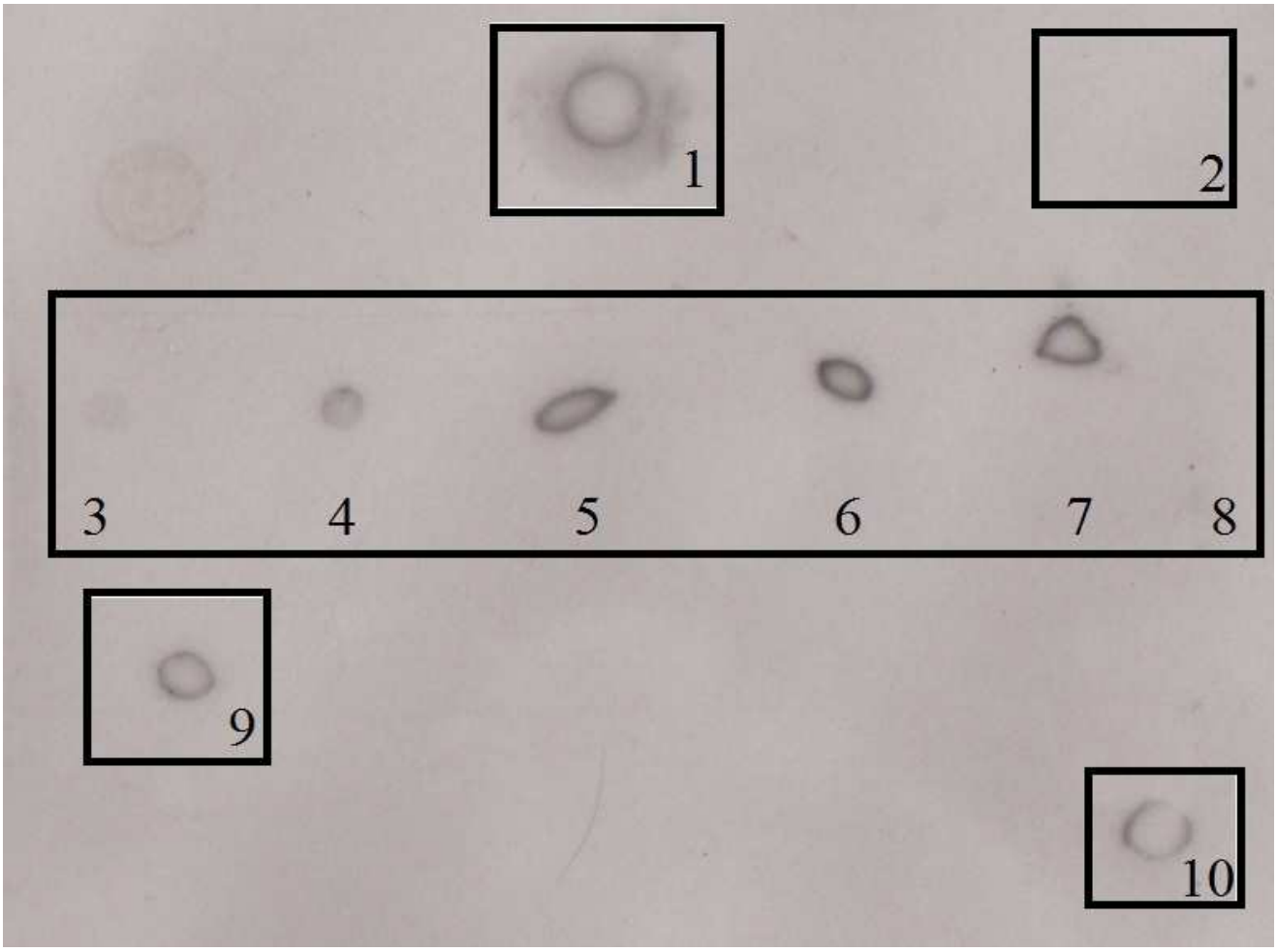

*Figure 1c. Sheep anti-TSST-1 conjugated to goat anti-sheep HRP antibody to was used to detect the presence of TSST-1 after being passed over an avidin column containing bound DR*201 as assumed in figure 1b. Sample 1 shows TSST-1 directly placed onto the membrane hybridizing to anti-TSST-1 antibody as expected. By contrast, sample 2 is purified DR*201, which shows no binding to anti-TSST-1, indicating that the polyclonal anti-TSST-1 antibody is specific to TSST-1. After DR*201 was bound to the avidin column as per protocol and TSST-1 added, the column was washed 6 times with PBS and collected. Samples 3-8, show that TSST-1 washed off the column and was subsequently detected via the anti-TSST-1 antibody. However, in the final wash, no significant amount of TSST-1 could be detected. This wash was assumed to contain no TSST-1 and was used as a negative control in subsequent PBMC expansion assays. After DR*201 was eluted as previously described, the eluate was assayed for the presence of TSST-1, shown in samples 9 and 10. This indicates that the TSST-1 remained bound to the avidin column. Because DR*201 remained bound to the avidin column via biotin, it is likely that the detection of TSST-1 is due to TSST-1 binding to DR*201 and was co-eluted*

*with DR*201. Thus, it was assumed that TSST-1 was bound to DR*201 consistent with the mechanism associated with superantigens. Although the elution profile in 3-8 is not what is typically seen during protein purification, this may be the result of an artifact as this finding could not be repeated in subsequent experiments, in which the amount of superantigen consistently declined as the column was washed.*

Figure 1. Purification and tetramerization of DR*201.

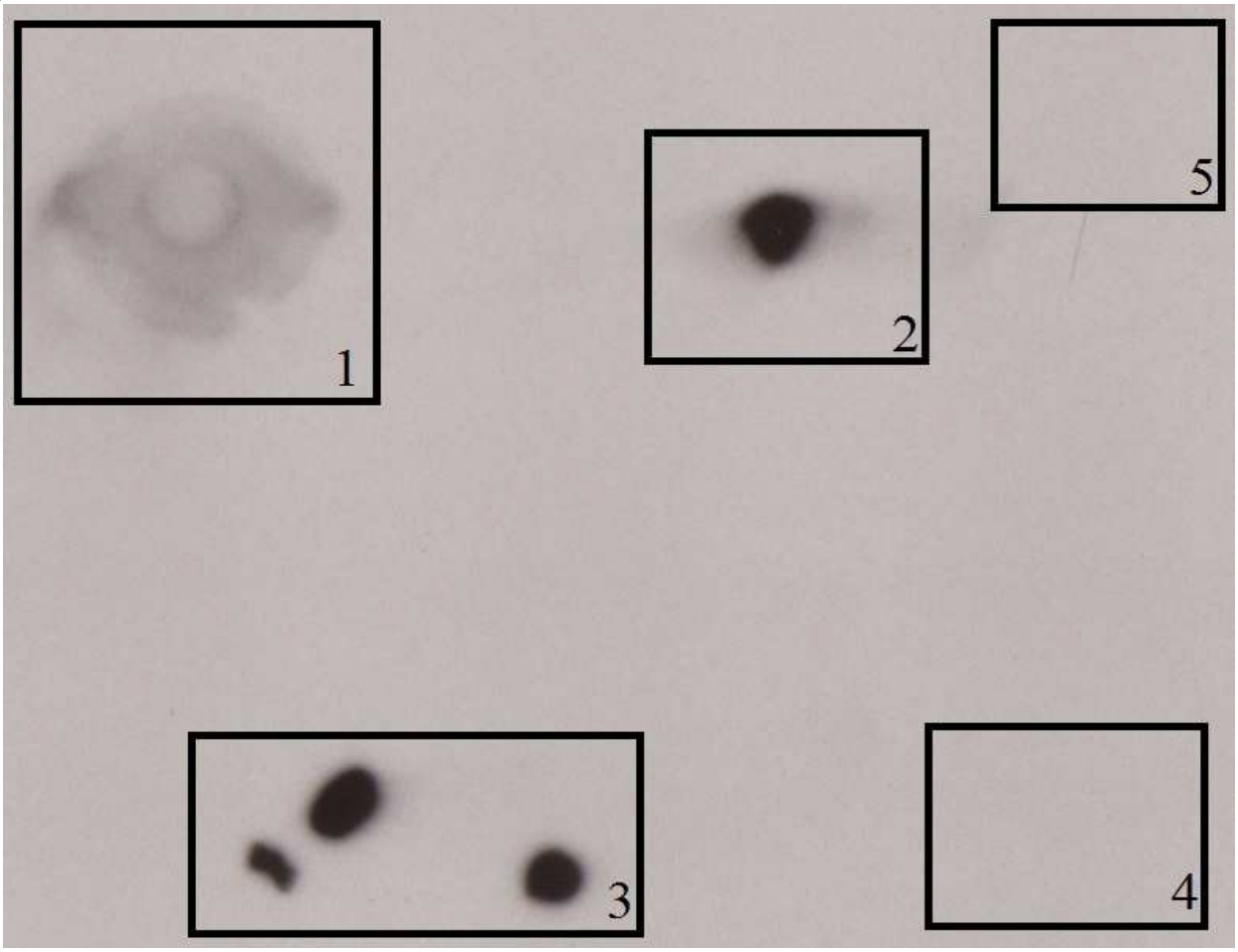

*Figure 1d. In this experiment, streptavidin was added to DR*20 at a 1:4 molar ratio to form the complete MHC-II tetramer. Since streptavidin has 4 separate biotin binding sites, a single molecule of streptavidin can bind to 4 molecules of biotinylated DR*201. The complex was then isolated by using a centrifugal filter unit with a pore size of 250 kDa. With a calculated molecular weight of 296,800 Dalton, the fully formed DR*201 should be retained against the filter, while free streptavidin and DR*201 should pass through the 250 kDa filter. These samples were probed with mouse anti-HLA-DR and visualized through goat anti-mouse HRP antibody. Samples 1 and 2 are the positive control, which is a solution of monomeric biotinylated and unbiotinylated DR*201 respectively. Sample 5 is 1% BSA, which serves as a negative control against anti-HLA-DR. Sample 3 is a solution of DR*201 and streptavidin that was incubated overnight at 4 ºC and then filtered against a 250 kDa filter. Sample 4 is the flowthrough solution from the 250 kDa filter. Sample 3 shows binding to anti-HLA-DR, indicating that some sort of process has occurred that has resulted in a high molecular weight aggregate being formed. Sample 4 shows no binding, indicating that most, if not all, of DR*201 was involved in this high molecular weight aggregate. Since DR*201 was biotinylated and streptavidin can theoretically*

*bind 4 molecules of DR*201, it was assumed that these high molecular aggregates were DR*201 tetramers. Although this is not conclusively proven, further experiments, depicted in figure 1e show that this mechanism is highly plausible.*

Figure 1. Purification and tetramerization of DR*201.

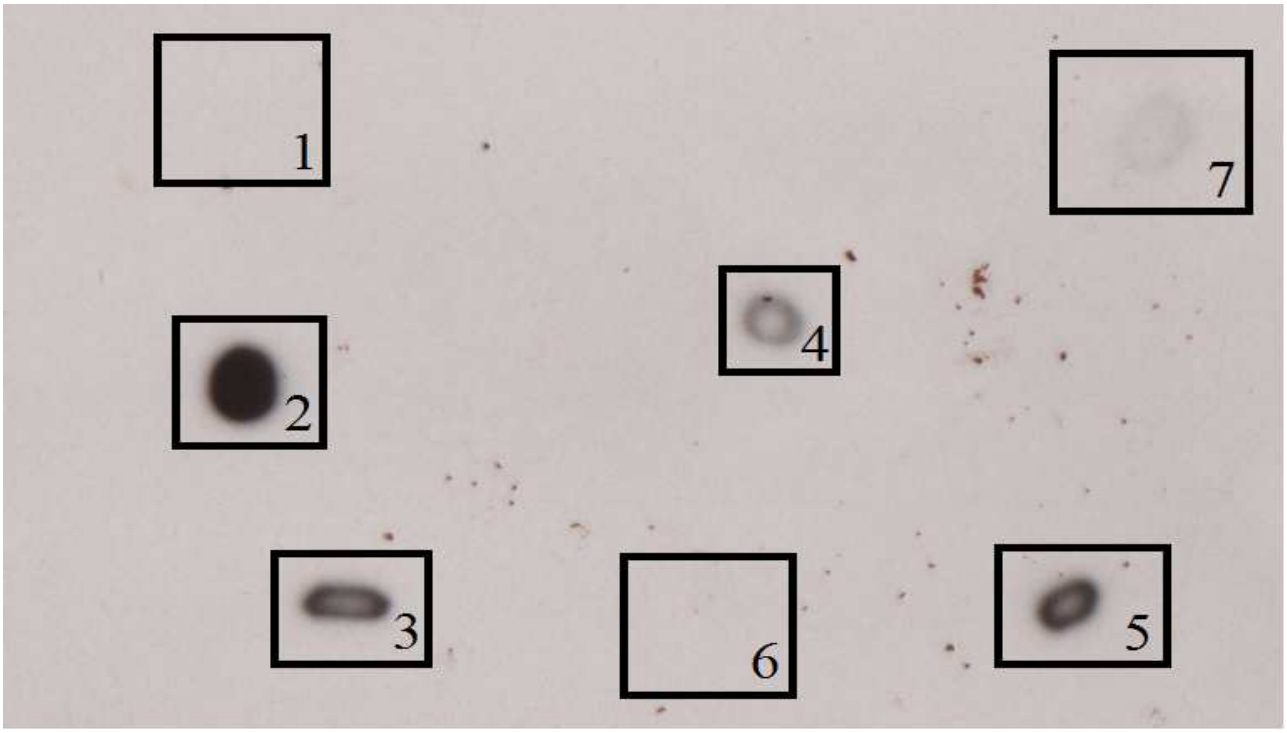

*Figure 1e. This experiment demonstrates that streptavidin is complexing with DR*201 in a specific manner, most likely due to streptavidin binding to biotin, which in turn is bound to DR*201. Mouse anti-HLA-DR conjugated to goat anti-mouse HRP antibody was used to determine the presence of DR*201 after several different treatments. Sample 1 is a solution of 1% BSA, showing no binding as expected. Sample 7 is a solution of DR*201, showing a signal, albeit weak, to the anti-HLA-DR antibody. Samples 2 and 3 are biotinylated DR*201 and biotinylated DR*201 bound to TSST-1, both complexed with streptavidin and filtered against a 250 kDa filter. When unbiotinylated DR*201 in a 1:4 molar ratio with streptavidin is passed through a 250 kDa filter, DR*201 can only be detected in the flowthrough solution, demonstrated in sample 4, while the retained solution is devoid of any DR*201, evidenced in sample 6. Sample 5 is unbiotinylated in a 1:4 molar ratio with streptavidin filtered against a 30 kDa filter, demonstrating that the 30 kDa filter is able to retain DR*201 while the 250 kDa filter allows DR*201 to pass through, even in the presence of streptavidin. This is highly suggestive that biotinylated DR*201 is complexing with streptavidin, forming the MHC-II tetramer.*

B. **DR*201 prevents T cell expansion in the presence of superantigens TSST-1 and SEB.**

In performing a PBMC culture to assess T cell proliferation via DR*201 binding, we expected to see that the interaction between DR*201 complexed with superantigen would result in expansion of T cells, as would be expected if only the superantigen alone was added to such cultures. However, as figure 2 demonstrates, this was not the case. For figure 2, all panels show cells after gating all PBMCs for lymphocytes via forward and side scatter, then gating lymphocytes on CD3-PeCy7 and CFSE. Figure 2a demonstrates that PBMCs treated with either the negative control or left untreated resulted in no proliferation of T cells, as would be expected. Although initially it was not known whether or not the negative control was truly negative, as we assumed that the absence of a signal from TSST-1 meant that the solution truly contained no superantigen molecules, the results of figure 2a show that our assumption was correct. It was observed that only 1.2% and 2.1% of T cells expanded in the negative control and untreated conditions respectively, as measured by a decrease in CFSE intensity. This was expected as no signal was given to these cells to expand. The addition of 100 ng/mL TSST-1 or SEB, shown in figures 2b and 2e, caused substantial T cell expansion. 15.6% and 22.3% of all T cells showed signs of expansion for PBMC cultures treated with 100ng/mL TSST-1 and SEB respectively. This was expected as the addition of a mitogen should result in proliferation of cells. Interestingly, PBMCs treated with 4 μg total protein of either DR*201:TSST-1 or DR*201:SEB, shown in figure 2c and 2d, show that this interaction does not result in T cells expanding, contrary to our expectations. A tentative calculation, assuming that all DR*201 binding sites were complexed with superantigen, suggests that approximately 1.46 μg of TSST-1 and 1.77 μg of SEB was present in the culture. This results in an approximate concentration of 7.3 μg/mL of TSST-1 and 8.83 μg/mL of SEB. Instead of

observing T cell expansion at levels comparable to the TSST-1 or SEB PBMC cultures, significantly less proliferation was observed, with 6.3% and 5.6% of T cells showing some signs of expansion in DR*201:TSST-1 or DR*201:SEB treated PBMCs. One drawback of this experiment was that total superantigen concentration was not quantified for DR*201 complexed with either TSST-1 or SEB. In order to calculate the amount of superantigen bound to DR*201, a known amount of DR*201 would have to be bound to an avidin column. Then, enough superantigen would be added to saturate the binding sites on DR*201 and a 1:1 molar ratio can be established through this interaction. Future experiments will have to quantify the amount of superantigen properly in order to interpret this data. However, at first glance, this experiment suggests that MHC-II complexed with superantigen may not be sufficient to expand T cells *in vitro*.

Upon examination of the data, we suspect that DR*201:TSST-1 and DR*201:SEB engages the TCR, however, the stimulation of the respective antigen presenting cell (APC) is absent. In this scenario, the T cell is primed to expand; however, the cell still has not received the necessary proliferation signals that would occur when MHC-II on the APC is stimulated through interacting with the TCR. Normally, the APC sends proliferation signals to the bound T cell via the physical interaction of CD80 and CD86 to CD28 and CTLA-4 as well as the release of cytokines, such as IL-4, 12, 15 and TGF-β (Melichar, *et. al.* 2000). In our system, the APC has been replaced with the DR*201 tetramer, removing a key component of the proliferation signaling system. Although this construct can, hypothetically, bind to T cells, the necessary signals for proliferation from the APC will be missing. Our initial assumption that DR*201 tetramer complexed with a superantigen would be sufficient at expanding T cells was not supported by the data. The addition of anti-CD28 and anti-CD3 antibodies

may be able to stimulate primed T cells to expand (Trickett, *et. al.* 2003). This modification may be able to meet the criteria for this assay to function as a screening tool for superantigens. This modification is predicated on DR*201:superantigen being able to prime a significant number of T cells for proliferation due to the strong binding between the TCR and DR*201 via the crosslinking action of the superantigen. In contrast, DR*201 tetramers will be unable to prime the vast majority of T cells due to inherently weak binding of DR*201 to the vast majority of T cells present in the cell culture. Therefore, with the addition of anti-CD3 and anti-CD28 antibodies, only DR*201 complexed with superantigen will induce measurable expansion of T cells as only these constructs will have the strong binding needed to prime bound T cells for proliferation.

Figure 2. DR*201 prevents T cell expansion in the presence of superantigens TSST-1 and SEB.

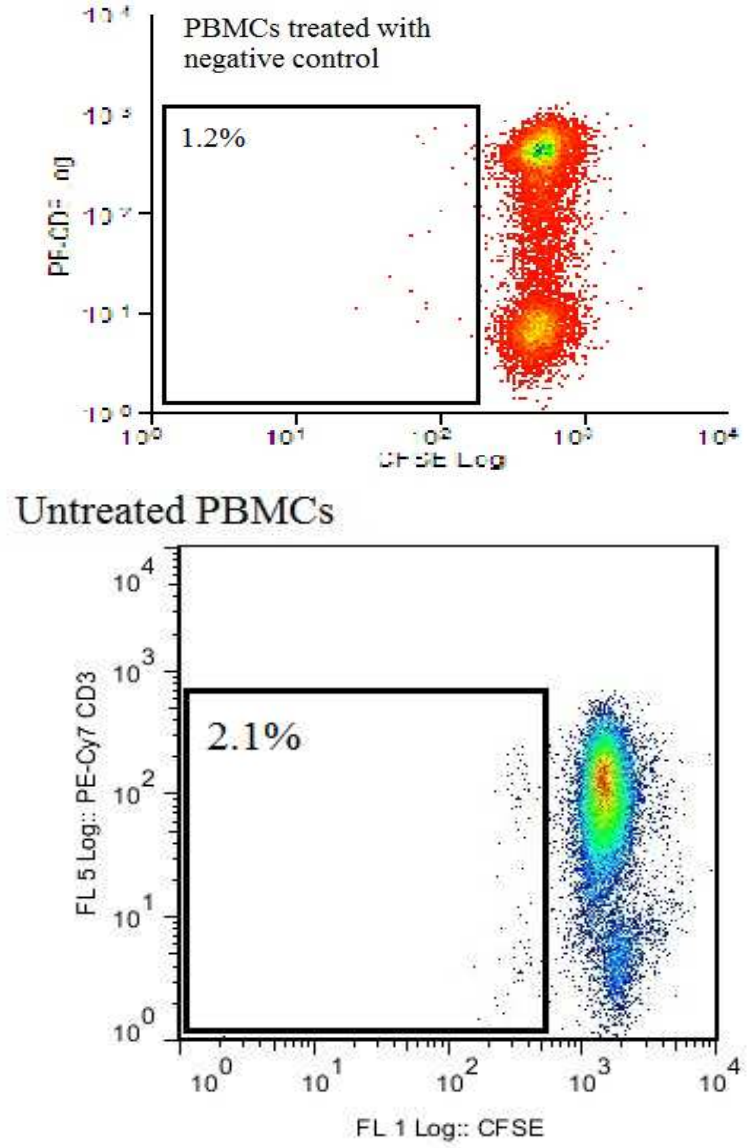

*Figure 2a. In this experiment, PBMCs were isolated and cultured as described previously. In first panel, PBMCs were treated with the negative control, described previously as the final PBS wash off the DR*201 avidin column treated with TSST-1. The total PBMC population was first gated on forward and side scatter to isolate the lymphocyte population. Then, the lymphocyte population was*

gated on CFSE and CD3-PeCy7. From figure 1c, it can be seen that very little to no TSST-1 could be detected in this wash. In the untreated condition, PBMCs were incubated with the addition of water equal to the volume added to the negative control PBMCs. The first panel, which represents the negative control treated PBMCs, shows only a small percentage, 1.2%, of cells have divided as assessed by reduction in CFSE staining intensity. The second panel, representing untreated PBMCs, also shows very little to no proliferation, at 2.1% as assessed by a reduction in the intensity of CFSE staining, as would be expected when neither antigen nor superantigen is added. Thus, we can conclude that the negative control is, in fact, a negative control as previously assumed.

Figure 2. DR*201 prevents T cell expansion in the presence of superantigens TSST-1 and SEB.

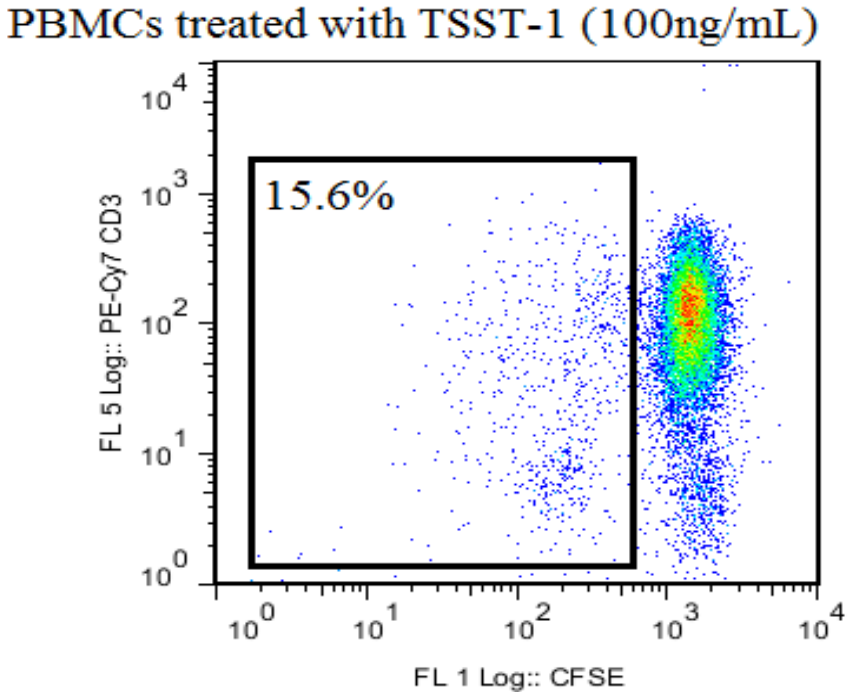

Figure 2b. When a total of 100ng/mL TSST-1 or SEB (Figure 2e) was added to PBMC culture, proliferation of T cells can be detected. The whole PBMC population was initially gated on forward and side scatter to identify the lymphocyte population. That lymphocyte population was then gated on CD3-PeCy7 and CFSE to assess T cell expansion. When gated on these channels, there is a population of T cells which show a decrease in the relative intensity of CFSE, indicating that these T cells have proliferated as would be expected when a mitogen such as TSST-1 or SEB is added to the tissue culture. 15.6% of T cells have proliferated as compared to only 2.1% and 1.2% T cells having proliferated in the untreated PBMCs and negative control cells respectively.

Figure 2. DR*201 prevents T cell expansion in the presence of superantigens TSST-1 and SEB.

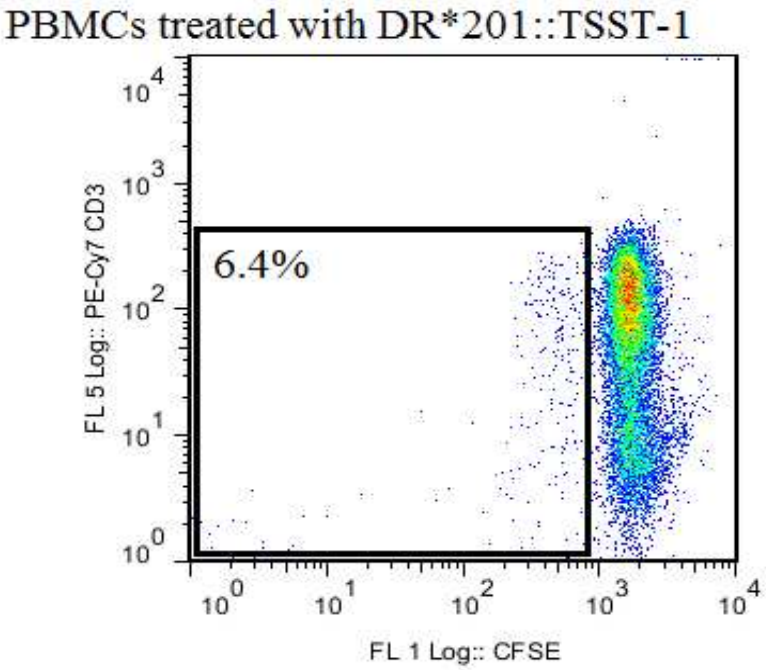

*Figure 2c. The lymphocyte population was identified by gating all cells on forward and side scatter as previously. These lymphocytes were then gated on CD3-PeCy7 and CFSE to analyze the T cell population in the tissue culture. Here, 4 μg total protein, compromised of DR*201 tetramer complexed with TSST-1, representing a tentative amount of 1.47 μg of TSST-1, was added to tissue culture. A marked decrease in T cell proliferation was observed. Here, 6.4% of T cells have proliferated as compared to the when TSST-1 was added to tissue culture and resulted in 15.6% of all T cell undergoing proliferation (Figure 2b). This indicates that DR*201 tetramer complexed with superantigen is unable to support T cells proliferation as previously hypothesized. Instead, a block on T cell proliferation was observed.*

Figure 2. DR*201 prevents T cell expansion in the presence of superantigens TSST-1 and SEB.

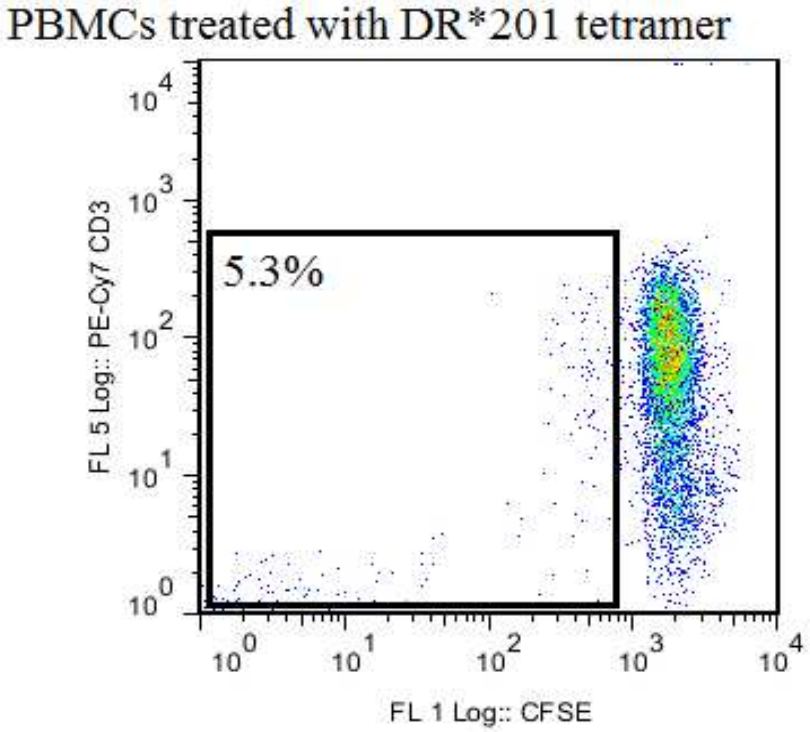

*Figure 2d. Total PBMCs were gated on forward and side scatter to isolate the lymphocyte population. Subsequently, lymphocytes were gated on CD3-PeCy7 and CFSE. Here we observe the lack of significant proliferation when 4 μg DR*201 tetramer was added to PBMC tissue culture. This was as expected as the DR*201:TCR interaction is too transient to induce proliferation in T cells. As the subcloned DR*201 is specific to Ag85, only T cells with TCRs able to recognize Ag85 will be able to bind tightly to DR*201 and proliferate, or be primed to proliferate.*

Figure 2. DR*201 prevents T cell expansion in the presence of superantigens TSST-1 and SEB.

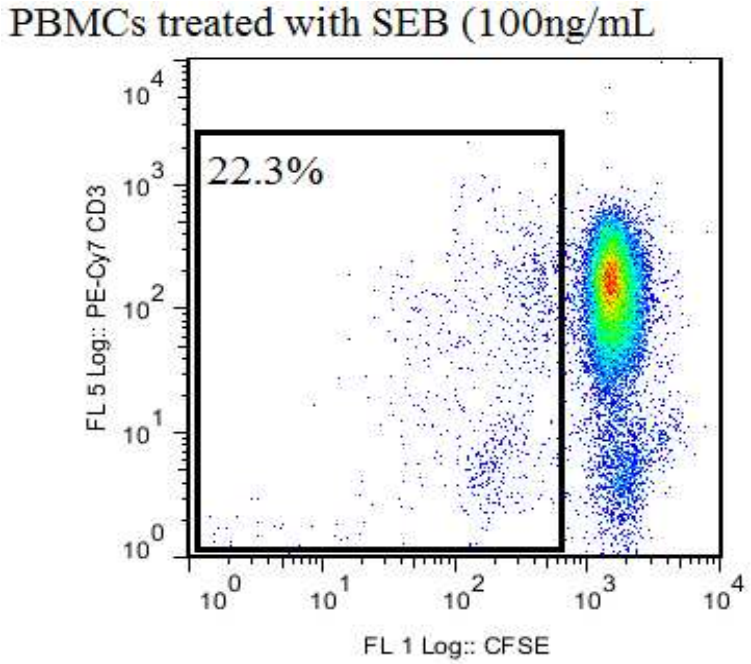

Figure 2e. The lymphocyte population was isolated as previously described, via side and forward scatter on the total PBMC population. These cells were then gated on CD3-PeCy7 and CFSE to assess T cell proliferation. Significant T cell expansion was observed with 22.3% of all gated cells having undergone proliferation. This was expected as the addition of a mitogen, such as SEB, is expected to induce non-clonal, non-specific T cell expansion.

Figure 2. DR*201 prevents T cell expansion in the presence of superantigens TSST-1 and SEB.

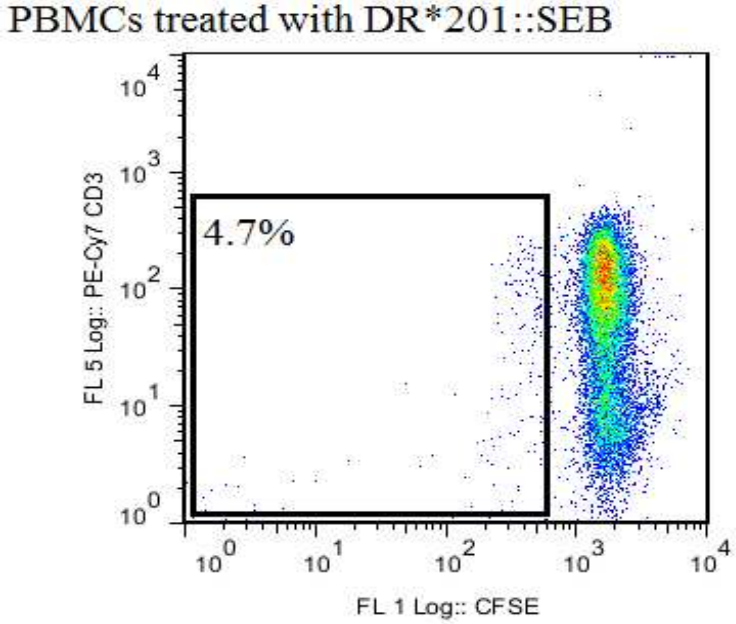

*Figure 2f. As before, the lymphocyte population was isolated according to forward and side scatter on the total PBMC population. Lymphocytes were then gated on CD3-PeCy7 and CFSE to assess T cell proliferation. As in figure 2c, when 4 µg total protein, consisting of DR*201 tetramer complexed to SEB, tentatively representing 1.77 µg of SEB, was added to PBMC tissue cultures, a marked decrease in T cell proliferation was observed. As compared to only SEB added to tissue culture, only 4.7% of cells have proliferated. This is a marked decrease from 22.3% in the superantigen only condition (figure 2e). This, along with the finding that DR*201:TSST-1 also inhibited T cell expansion suggests that MHC-II crosslinked to the TCR is not sufficient to induce T cell proliferation but that additional signals are also required.*

C. **IL-22 was successful subcloned and expressed by *Listeria monocytogenes.***

In order to subclone IL-22 into *L. monocytogenes,* PCR was performed to amplify IL-22 from *Lactococcus lactis* plasmids containing the IL-22 gene. Primers were designed to amplify the IL-22 gene as well to modify the restriction enzyme sites to BamHI and SpeI to facilitate subcloning into the plasmid pPL6. Figure 3a shows the successful amplification of IL-22 from *L. lactis*. If amplification is successful, an amplicon of approximately 500 basepairs should be detected. Wells 1-5 show amplification of IL-22 from 5 different *L. lactis* clones while the 6th band is a positive control using the original primers designed to subclone IL-22 into *L. lactis*. All wells show the expected amplicon size of approximately 500 basepairs, suggesting that PCR was successful in amplifying the IL-22 gene. Well 8 is the water negative control. Furthermore, the restriction enzyme sites were successfully modified as indicated by Figure 3b. Here, pPL6 and IL-22 were digested with BamHI and SpeI sequentially and then ligated using T4 ligase as previously described. After transformation of *E. coli* TOP 10 cells, 14 clones were picked and tested for the IL-22 insert. The clones were isolated for their plasmid DNA and then PCR was performed using the same IL-22 primers as in Figure 3a. As can be seen, each transformant contained the IL-22 gene, while lane 16 and 17 show neither pPL6 nor water produce the amplicon of interest.

Once pPL6 containing IL-22 was successfully identified, the pPL6 plasmid was transferred from *E. coli* TOP10 to *E. coli* SM10 via heat-shock transformation. SM10 cells were mated with the following *Listeria monocytogenes* strains: wild-type, ΔactA, NF-972 (genotype: ΔactA, constitutively active transcription factor prfA [prfA*]), NF-974 (genotype: ΔactA, prfA*), using the conditions as described previously. Figure 3b shows that the mating of pPL6-IL-22 from *E. coli* SM10 cells into *L.*

monocytogenes was successful. After isolation of genomic DNA from transformed *L. monocytogenes,* PCR was performed to test for the presence of the IL-22 gene. As expected, when pPL6-IL-22 was transformed into the wild-type, ΔactA, NF-972, and NF-974 strains, they were positive for the IL-22 gene as amplified by both IL-22 primers (figure 3c). As can be seen, an insert of approximately 500 can be detected when PCR was performed using the IL-22 primers. When the empty pPL6 vector or non-transformed *L. monocytogenes* genomic DNA was amplified, no IL-22 amplicon could be detected (figure 3c).

To determine whether or not IL-22 was secreted successfully into the environment, *L. monocytogenes* supernatants from mutants transformed with pPL6 or pPL6-IL-22 were collected and processed as described previously. *L. monocytogenes* was grown overnight at 37ºC in BHI supplemented with chloramphenicol at 15 μg/mL. As subcloned, IL-22 is approximately 20kDa. The supernatants were concentrated against a 10 kDa centrifugal filter unit to retain the IL-22 protein against the filter. The retained solution was then processed according to standard Western blotting protocol. After a Western blot of the proteins was performed, IL-22 was shown to be secreted into the medium as hypothesized. As can be seen in Figure 3d, *Listeria monocytogenes* strains transformed with pPL6-IL-22 successfully secreted IL-22 into the medium while those with the empty vector pPL6 or non-transformed *L. monocytogenes* did not secrete IL-22. This experiment confirms that *Listeria monocytogenes* can be used as an expression vehicle for secreting proteins into the extracellular environment. The hly promoter and subsequent downstream sequences promote secretion of proteins into the supernatant (Yan, *et. al.* 2008). Normally, this promoter is responsible for the transcription of Listeriolysin O, which is then secreted into the extracellular environment. By placing the IL-22 gene

under the control of the hly promoter, we have co-opted the bacteria's natural machinery to secrete proteins to suit our needs. Thus, as figure 3d demonstrates, IL-22 can be detected in the extracellular environment, confirming that IL-22 is secreted rather than stored within the bacterial cell.

Figure 3. IL-22 was successful subcloned and expressed by *Listeria monocytogenes.*

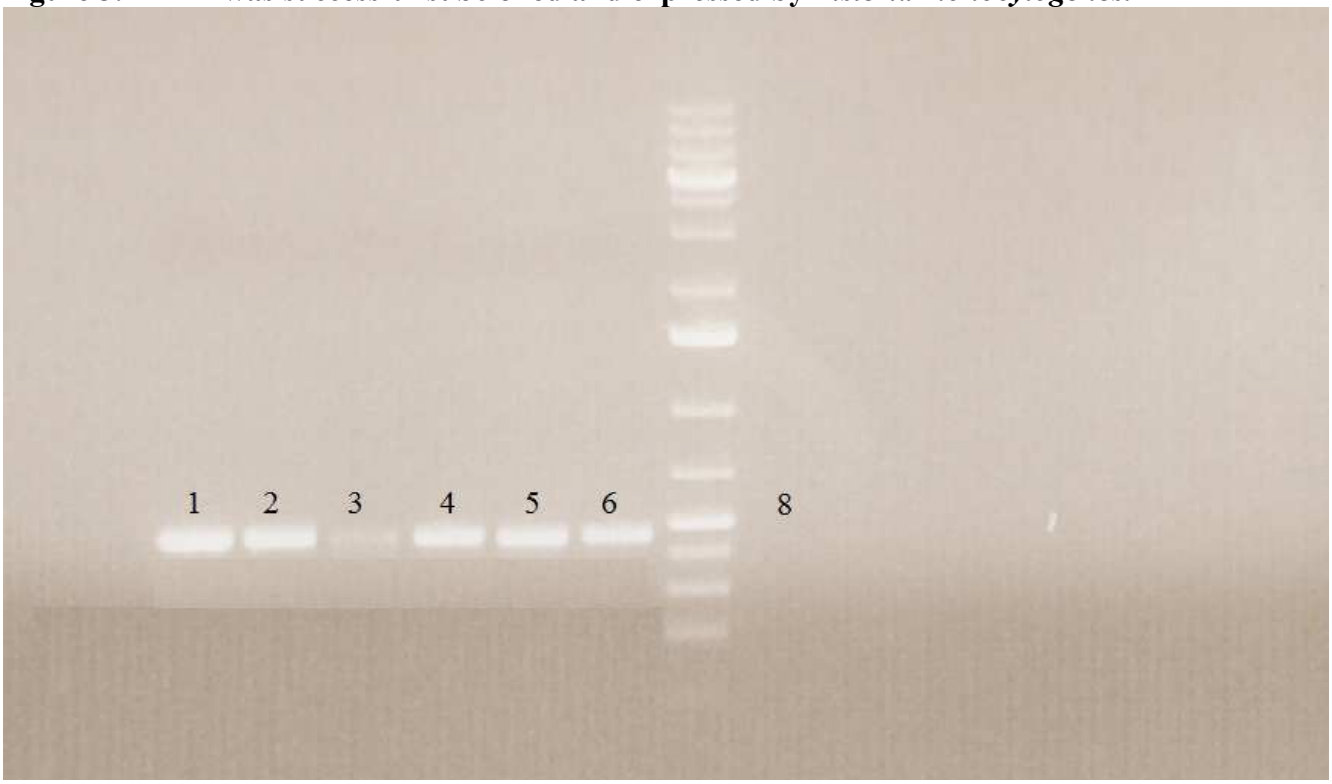

Figure 3a. The successful amplification of IL-22 from L. lactis *pXmH is shown in wells 1-7. This plasmid contains IL-22 flanked by XbaI and HindIII restriction enzyme sites. Primers were used to amplify IL-22 as well as change these restriction sites to BamHI and SpeI as described in the methods. The first 5 wells show successful amplification of IL-22 from* L. lactis *pXmH clones with primers that modify the restriction enzyme sites. Well 6 shows the amplification of IL-22 from pXmH with the original primers that were used to subclone IL-22 into pXmH. An expected band of approximately 500 basepairs is seen in all 6 wells, confirming that the PCR reaction was successful. Well 8 is the negative water control, showing no amplification as expected.*

Figure 3. IL-22 was successful subcloned and expressed by *Listeria monocytogenes.*

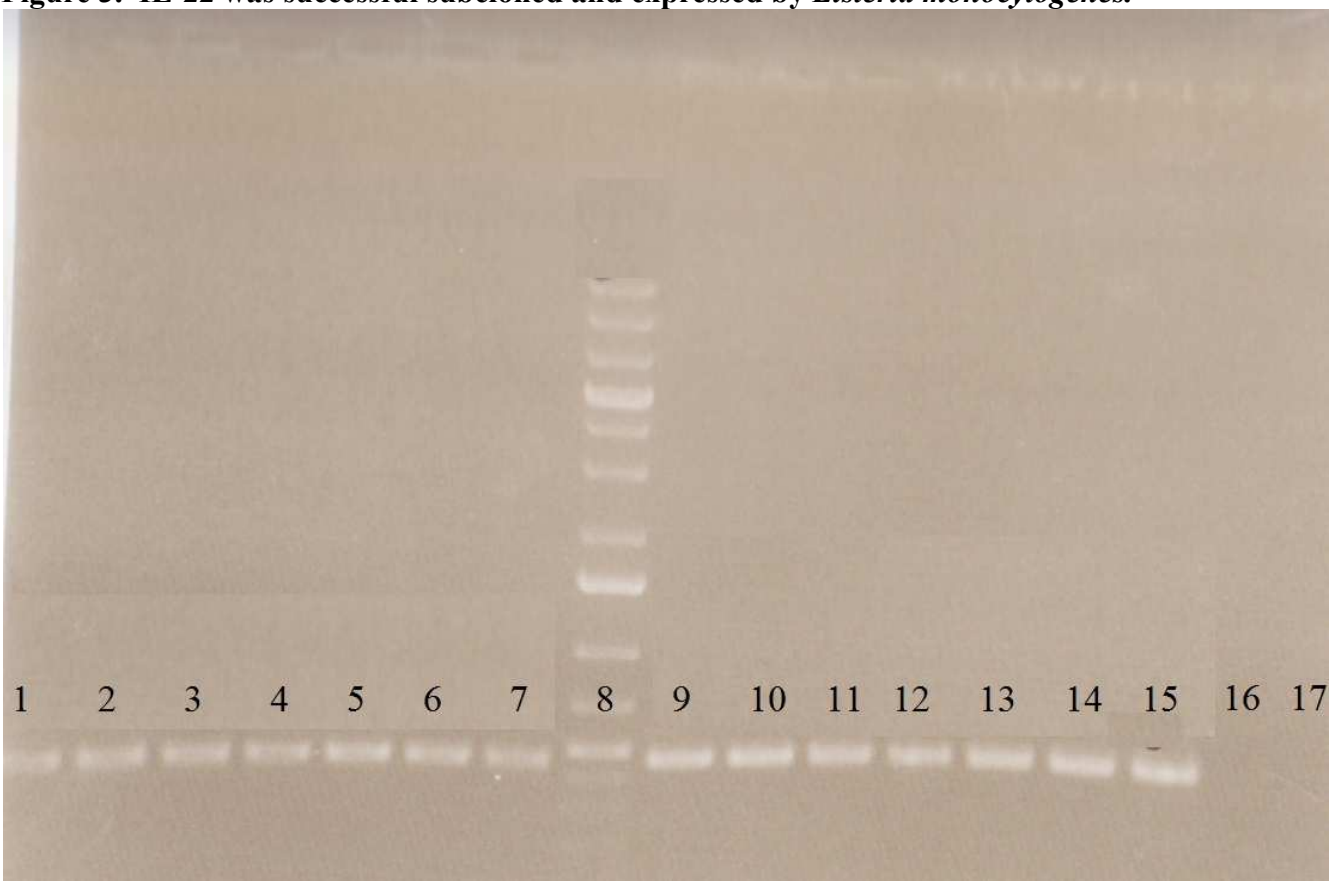

Figure 3b. Here, the successful amplification of IL-22 after it has been digested with BamHI and SpeI sequentially, ligated into pPL6, then transformed into E. coli *TOP10 is demonstrated. Wells 1-7 and 9-14 show the amplification of IL-22 after being isolated from transformed* E. coli *TOP 10* cells. *Well 15 is the positive control, that is, amplification of isolated pXmH containing IL-22. Well 16 is the amplification of the empty vector pPL6 while well 17 is the negative water control showing an absence of DNA, as expected.*

Figure 3. IL-22 was successful subcloned and expressed by *Listeria monocytogenes.*

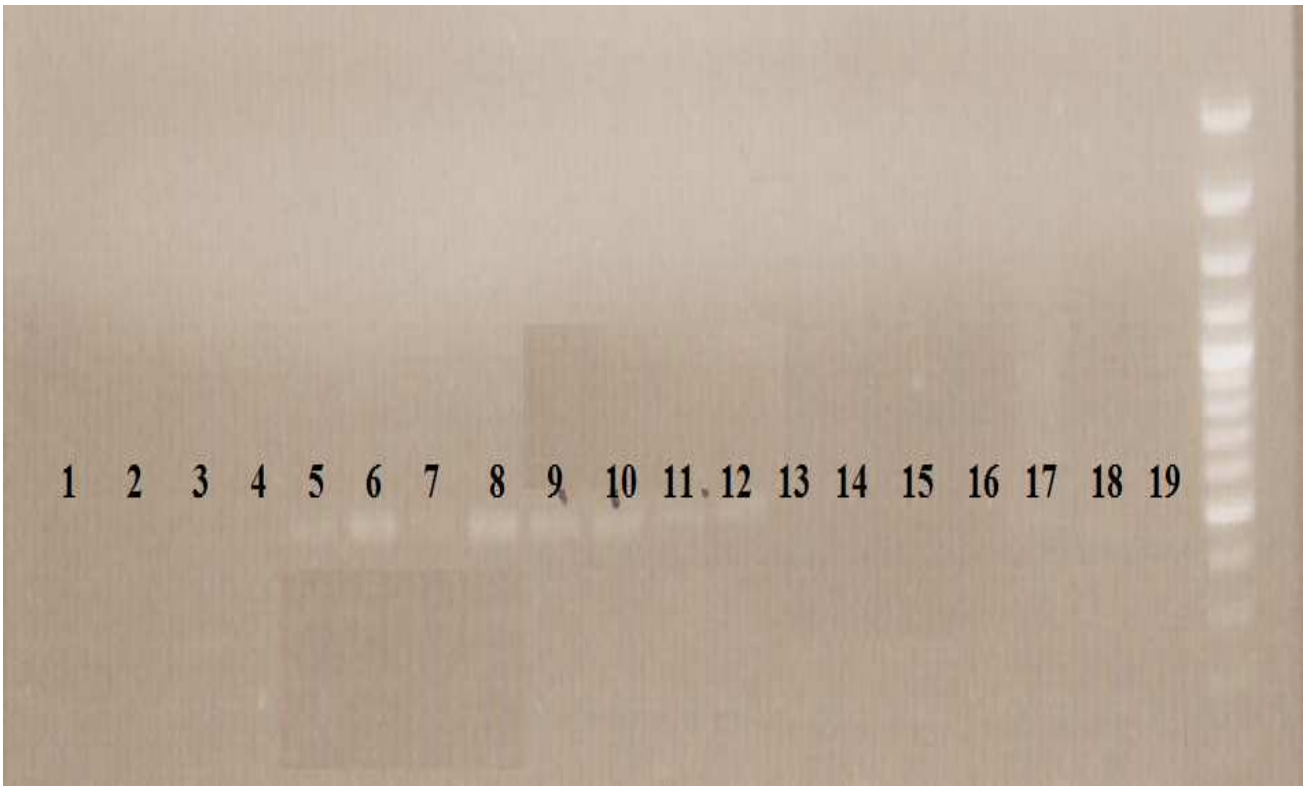

Figure 3c. This experiment shows the amplification of IL-22 from isolated genomic DNA from L. monocytogenes *strains that were transformed.* E. coli *SM10 cells were transformed with the plasmids containing IL-22 as demonstrated in figure 3b and then mated with* L. monocytogenes*. The cells were then plated on double selective plates, streptomycin and chloramphenicol. Two resulting colonies from each* L. monocytogenes *strains were then picked and analyzed for the presence of the IL-22 gene. Wells 1-4 are the results of PCR of the IL-22 gene in the wild-type, ΔactA, 972 and 974* L. monocytogenes *strains that were not transformed; these show no amplification as expected. Wells 5-12 are the results of PCR on presumptive* L. monocytogenes *transformants. An amplicon of the correct size is detected in each case; the strains are wild-type, ΔactA, 972 and 974 respectively for wells 5-8 and wild-type, ΔactA, 972 and 974 respectively for wells 9-12. Wells 13-16 are the empty vector controls for the wild-type, ΔactA, 972, and 974 respectively, showing no amplification of IL-22 as expected. Wells 17, 18, and 19 are the negative water controls, again showing no amplification of DNA.*

Figure 3. IL-22 was successful subcloned and expressed by *Listeria monocytogenes.*

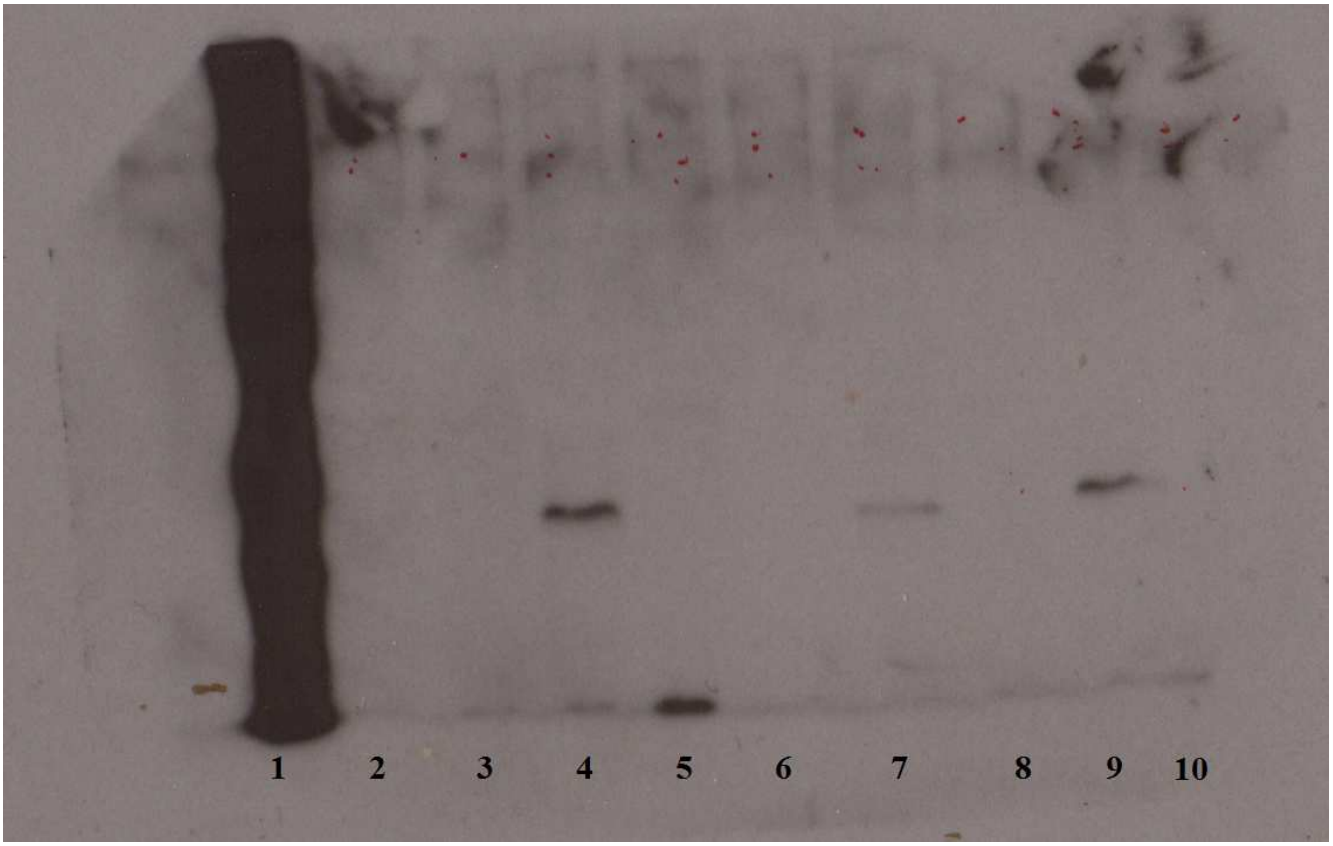

Figure 3d. Figure 3d demonstrates that the IL-22 is successfully expressed and secreted into the environment by Listeria monocytogenes *strains bearing the IL-22 integration via pPL6 as determined by binding via an anti-cmyc antibody. Lanes 4, 7 and 9 are the* L. monocytogenes *strains bearing the IL-22 gene and are the wild-type, 972 and 974 strains respectively. Lanes 2, 3 are the wild-type and ΔactA strains respectively, while 5 and 6 are 972 and 974 strains. Finally, lane 8 and 10 are the 972 and 974 strains transformed with pPL6 with no insert. Processed IL-22 has an approximately molecular weight of 20 kDa, which agrees with the bands in lanes 4, 7 and 10. The spurious binding in lane 5 near the bottom could not be replicated and may be the dye front causing non-specific binding to occur.*

D. **IL-22 expression does not stimulate Vγ2Vδ2 T cell expansion in *in vitro* PBMC culture.**

To assess whether or not *Listeria* infected THP-1 macrophages are able to stimulate Vγ2Vδ2 expansion with *Listeria* derived IL-22, THP-1 macrophages were infected at a 1:1 MOI with the wild-type, ΔactA, NF-972-pPL6 and NF-972-pPL6-IL-22. After the addition of gentamicin sulfate to kill any extracellular bacteria, the macrophages were incubated at a 50:1 ratio with Ficoll isolated PBMCs for 7 days. IL-2 was added to the culture at a final concentration of 100U/mL. On day 3, half the media was removed and fresh media was added to the culture. Enough IL-2 was added to the culture to maintain the concentration at 100U/mL; it was assumed that half the IL-2 was lost due to the changing of the media. Figure 4a shows the baseline levels of Vγ2Vδ2 T cells in the context of untreated PBMCs and PBMCs treated with uninfected THP-1 macrophages. For this experiment, all panels were gated on side and forward scatter to isolate the lymphocyte population. These isolated lymphocytes were then gated on CD3-PeCy7 and Vγ2-AlexaFluor680. Quadrants R2 and R4 represent the total number of CD3- cells, with the proportion represented in R4 while quadrants R5 and R8 represent the total number of CD3+ T cells with the proportion in R5. Quadrant R8 represents the total number of Vγ2Vδ2+ CD3+ T cells and the proportion of Vγ2Vδ2 CD3+ cells represented in R8. Both panels show similar results, with approximately 60% of all lymphocytes being CD3- and Vγ2Vδ2 T cells compromising 6% and 4% in the untreated PBMC and PBMCs treated with uninfected macrophages conditions respectively. However, alloreactivity may be causing cell death as the total cell number is markedly decreased when PBMCs are incubated with THP-1 macrophages. This effect was seen throughout the experiment.

When wild-type *Listeria* infected THP-1 macrophages were incubated with rhesus-derived PBMCs, a significant amount of cell death was observed. This was to be expected as wild-type *Listeria* would have been able to spread cell-to-cell. Moreover, when the supernatant was observed, significant amounts of bacterial growth could be seen. This was in contrast to all other conditions, where the supernatant was free of bacterial growth. This is likely due to cell lysis and subsequent release of bacteria. CD3+ lymphocytes were observed to compose 32.8% of the total lymphocyte population and Vγ2Vδ2 T cells were 3.2% of the total CD3+ population. When ΔactA infected macrophages were incubated with PBMCs, there is a slight biased towards CD3+, with 47.8% of the total lymphocyte population being CD3+. The total number of Vγ2Vδ2 T cells was relatively similar, with 7.7% of CD3+ lymphocytes being Vγ2Vδ2 T cells.

When NF-972-pPL6 infected macrophages were incubated with PBMCs, a strong bias towards CD3+ T cells was observed with 66.3% of the total lymphocyte population being positive for CD3. This was not expected and we hypothesize that the overproduction of certain immunogens, due to the activity of constitutively PrfA, is responsible for this observation. The total number of Vγ2Vδ2 T cells was unchanged with the total population of Vγ2Vδ2 standing at 6.9% of all CD3+ lymphocytes. When NF-972-pPL6-IL-22 infected macrophages were incubated with PBMCs, the same bias towards CD3+ lymphocytes was observed, however, the percentage of Vγ2Vδ2 T cells remained unchanged with only 8.1% of all CD3+ lymphocytes being positive for the Vγ2 marker. This experiment, although not conclusive, suggests that IL-22 has a minor role, if any, in the expansion of Vγ2Vδ2 T cells in the context of *Listeria monocytogenes* infection in PBMC culture.

Figure 4. IL-22 expression does not stimulate Vγ2Vδ2 T cell expansion in *in vitro* PBMC culture.

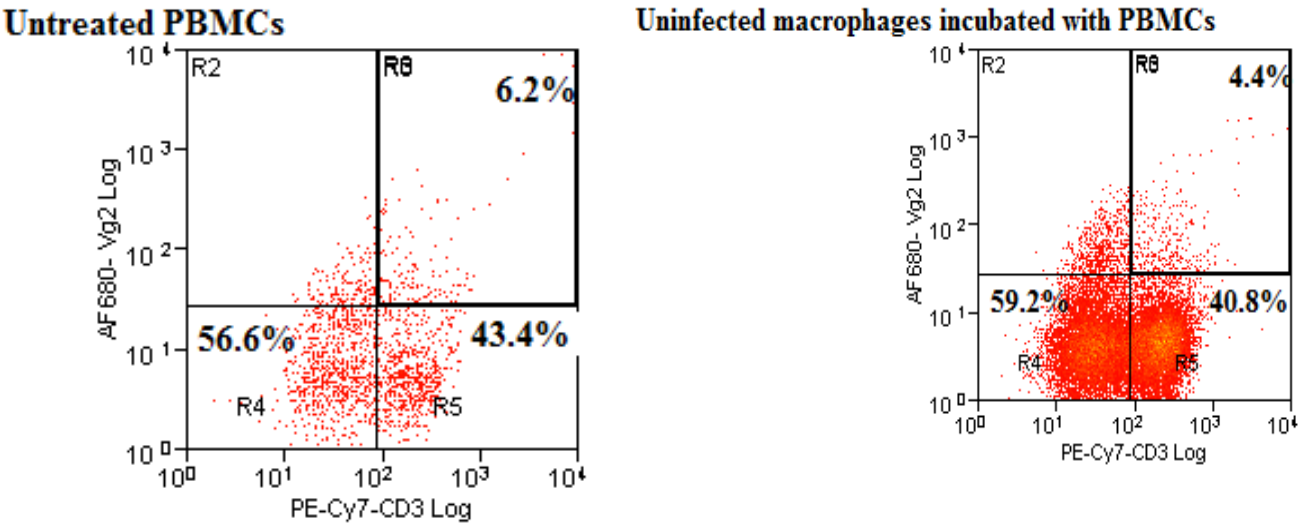

Figure 4a. In these panels and all subsequent panels, total PBMCs were gated on side and forward scatter to identify the lymphocyte population. Then, the lymphocytes were gated on CD3-PeCy7 and Vγ2-AlexaFluor680 to identify the Vγ2Vδ2 population. For this figure and subsequent figures, quadrants R2 and R4 represent the total number of CD3- cells, with the proportion represented in R4 while quadrants R5 and R8 represent the total number of CD3+ T cells with the proportion in R5. Quadrant R8 represents the total number of Vγ2Vδ2+ CD3+ T cells and the proportion of Vγ2Vδ2 CD3+ cells represented in R8. Here, untreated PBMCs and PBMCs incubated with uninfected THP-1 macrophages were examined to establish the baseline control population. Neither population shows an increase in the proportion of Vγ2Vδ2 T cells, which normally compromise between 4% and 7% of the resting peripheral population. Here, 6.2% and 4.4% of CD3+ T cells, in untreated PBMCs and PBMCs treated with uninfected macrophages respectively, are positive for Vγ2, a marker for Vγ2Vδ2 T cells. Although the cell number is significantly higher when PBMCs are incubated with THP-1 macrophages, this may be to due to alloreactivity as the PBMCs and THP-1 macrophages are unlikely to share the same MHC-II locus.

Figure 4. IL-22 expression does not stimulate Vγ2Vδ2 T cell expansion in *in vitro* PBMC culture.

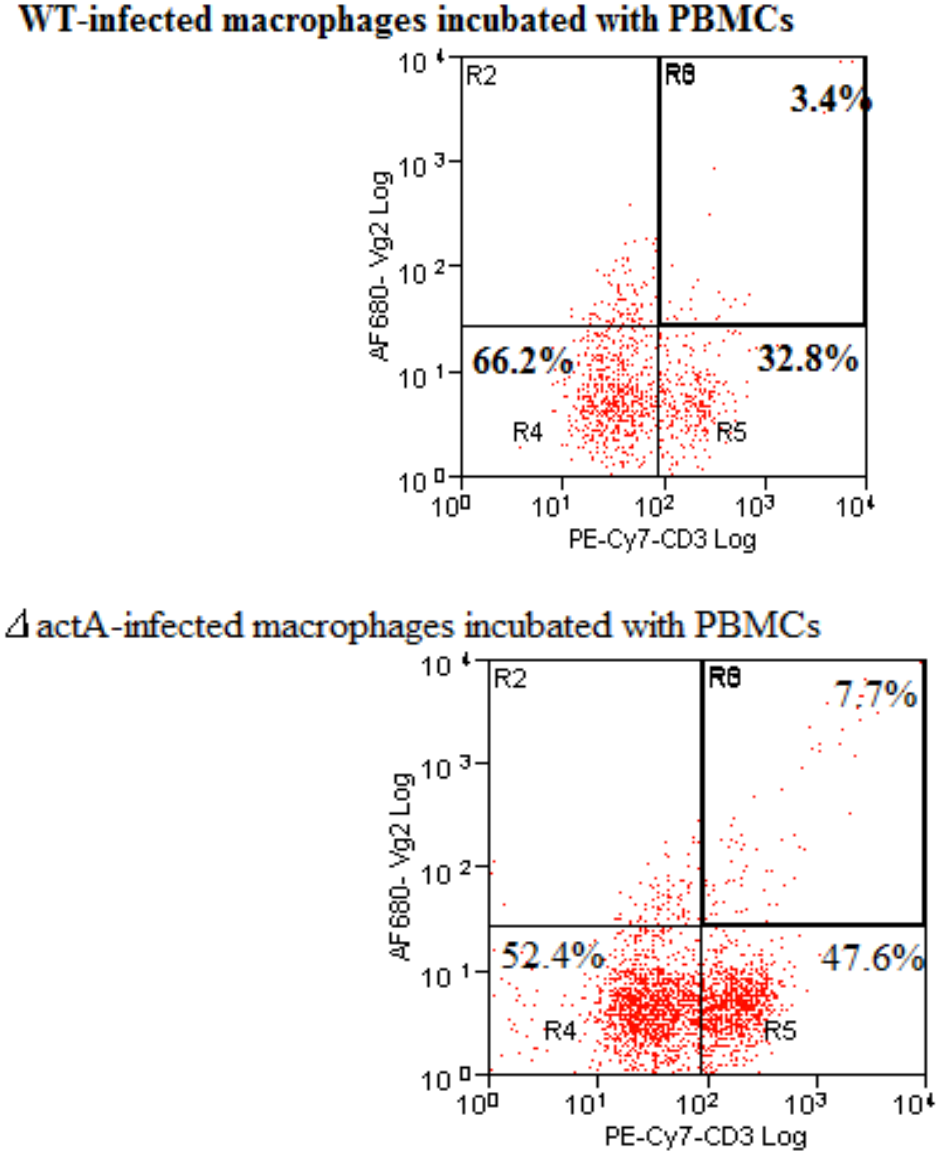

Figure 4b. When PBMCs are incubated with THP-1 macrophages previously infected with wild-type Listeria monocytogenes, *no significant expansion of Vγ2Vδ2 T cells is noted. In fact, the proportion of Vγ2Vδ2 decreased slightly. Furthermore, a significant reduction in lymphocytes is noted and is expected as the wild-type bacteria can spread cell-to-cell and result in the cell death observed.*

A slight bias towards CD3- lymphocytes is observed, with 66.2% of the total lymphocyte population being CD3however it is not known whether or not this bias is significant.

When ΔactA knockout mutants are infected with THP-1 macrophages and co-cultured with PBMCs, Vγ2Vδ2 cell expansion is slightly enhanced, although this increase is not significantly different than the normal resting population in the periphery. As expected, cell numbers are significantly higher and this is can be explained by the fact that ΔactA mutants are approximately 1000-fold less infectious than the wild type. This is evident by the larger number of lymphocytes that are both CD3+ and CD3- as compared to the Listeria *wild-type infection condition. Overall, 7.7% of CD3+ T cells were Vγ2Vδ2 positive while 47.6% of all lymphocytes were CD3+.*

Figure 4. IL-22 expression does not stimulate Vγ2Vδ2 T cell expansion in *in vitro* PBMC culture.

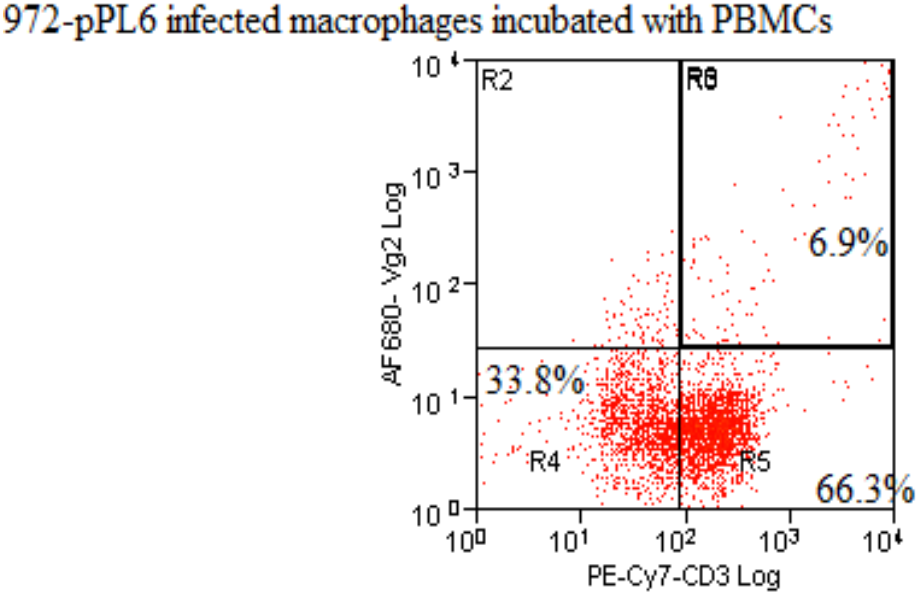

Figure 4c. This is the prfA empty vector control, in which the 972 strain was infected with THP-1 macrophages and then co-cultured with rhesus monkey PBMCs. As the 972 strain is also an ΔactA knockout, a similar pattern of cell survival and Vγ2Vδ2 expansion is observed. Interestingly, the number of CD3+ T cells is increased in this culture condition; here CD3+ lymphocytes compromise 66.3% of all lymphocytes as compared to 32.8% and 47.6% in the wild-type and ΔactA knockout strain respectively and 40.8% in the uninfected controls. This suggests that the overexpression of* Listeria *immunogens, due to the constitutive activity of prfA, results in a biasing towards CD3+ lymphocytes. Vγ2Vδ2 T cells were not significantly overrepresented in this culture, with 6.9% of all CD3+ lymphocytes bearing the Vγ2 marker.*

Figure 4. IL-22 expression does not stimulate Vγ2Vδ2 T cell expansion in *in vitro* PBMC culture.

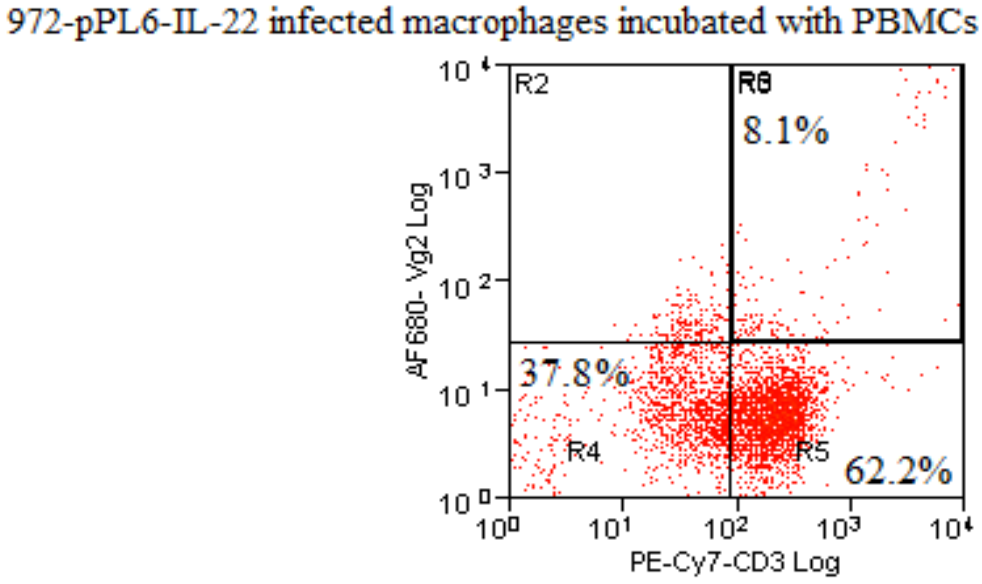

Figure 4d. Here, it was shown the effect of expressed IL-22 via the Listeria *expression vehicle in infected macrophages co-cultured with rhesus monkey PBMCs do not induce Vγ2Vδ2 T cell expansion.. A similar pattern of lymphocyte composition and Vγ2Vδ2 expansion is seen as with the 972 empty vector control as well as the ΔactA knockout strain. A significant increase in CD3+ T cell numbers is seen as compared to CD3- in which CD3+ cells compromise 62.2% of the total lymphocyte population. This bias towards CD3+ lymphocytes is most likely due to the activity of prfA and not IL-22 because this effect is also seen in the 972 empty vector. Thus, we hypothesize that some overexpressed immunogen is responsible for the biasing of lymphocytes towards being CD3+. 8.1% of CD3+ cells were Vγ2+, which is comparable to the 972-pPL6 and ΔactA knockout controls, suggesting that IL-22 plays a minor role, if any, in expanding Vγ2Vδ2 T cells under these culture conditions.*

IV. Discussion

The versatility of MHC-II tetramers guided our search for a hypothesized *M. tuberculosis* superantigen. We reasoned that crosslinking of DR*201 to the TCR would be enough to induce indiscriminate proliferation of T cells. However, our results indicate that this is not the case. Instead, it seems that additional signals are necessary to induce T cell proliferation beyond TCR stimulation via superantigen crosslinked MHC-II interaction. Although we suspect that the DR*201 tetramer is able to bind to T cells, the absence of signals from the corresponding APC results in T cells not responding appropriately to TCR stimulation. It is hypothesized that the addition of anti-CD3 or anti-CD28 antibodies is necessary to induce widespread T cell proliferation (Trickett, *et. al.,* 2003). Normally, CD3 and CD28 stimulation occurs in the context of antigen presentation upon tight TCR to MHC-II binding. This combination of signals induces the proliferation of antigen-specific T cells in response to an antigen. Since superantigens crosslink the TCR to MHC-II, it is probable that this interaction induces the APC to stimulate CD3 and CD28 as well as secrete pro-growth cytokines, thus causing proliferation of every T cell that was crosslinked via superantigen. When anti-CD3 and anti-CD28 antibodies are added to T cells primed with DR*201 tetramers, these primed cells may expand. However, DR*201 binding to TCR must be put into context. Only those T cells with TCRs specific to DR*201-Ag85 will bind tightly to the tetramer and thus will be stimulated to proliferate. The total number of T cells that satisfy this criterion will be extremely small; in fact, only a handful of T cells in the entire periphery may meet this criterion Therefore, we expect at least 100-fold less expansion of T cells when anti-CD3 and anti-CD28 antibodies are added to DR*201 tetramer stimulated T cells. In

contrast, DR*201 crosslinked to the TCR via superantigen and stimulated with anti-CD3 and anti-CD28 antibodies will induce the indiscriminate proliferation of every T cell with a crosslinked TCR. As a result, large numbers of T cells will be observed to proliferate when anti-CD3 and anti-CD28 antibodies are added to the PBMC culture. With this modification to the protocol, we hypothesize that DR*201 tetramer technologies will enable us to probe for *M. tuberculosis* superantigens.

In addition to precisely identifying the necessary conditions to induce T cell proliferation, we also have to demonstrate that DR*201 can selectively bind superantigens in a complex sample. In theory, the majority of proteins will be unable to bind to DR*201; only superantigens will able to bind to the DR*201 tetramer. This study only showed that DR*201 can potentially bind to superantigen when that superantigen was provided in a pure sample. Showing that DR*201 can preferentially bind superantigens in a complex sample has yet to be demonstrated. By incubating DR*201 with a complex mixture containing superantigens, we can demonstrate that selective binding of superantigens is possible. *Staphylococcus aureus* is able to produce superantigens while cultured in broth (Schlievert *et. al.* 2009). By taking *Staphylococcus aureus* cells and supernatants, isolating the protein fractions and then using DR*201 to selectively purify out the superantigens of interest, we can demonstrate that this protocol can purify superantigens preferentially in a complex mixture.

The use of *Listeria monocytogenes* as a vehicle to express proteins within infected cells allows us to investigate the role of IL-22 in the context of infection. IL-22 has dual functions as both a pro-inflammatory cytokine as well as a suppressor of immune responses (Xie, *et. al.,* 2000). As a result, the precise mechanism of action during infection is not known. In addition, evidence exists that IL-22 can be produced by Vγ2Vδ2 T cells (Ness-Schwickerath *et. al.,* 2010). Vγ2Vδ2 T cells respond to

phosphoantigens, such as HMBPP, produced during the course of bacterial infection (Wang, *et. al.*, 2010). This is significant because Vγ2Vδ2 T cells can expand in the context of bacterial infections and modulate the adaptive and innate immune responses. Our laboratory has demonstrated that Vγ2Vδ2 T cells can compose a significant portion of the total T cell population in both the periphery as well as infected tissue in *M. tuberculosis* infection (Yao *et. al.*, 2008, unpublished data). Investigating the role of IL-22 and Vγ2Vδ2 T cell expansion will enhance our knowledge of how the immune system is able to initiate and modulate an immune response.

This study investigating IL-22 and Vγ2Vδ2 expansion is preliminary, however, one observation is that PrfA* mutants, when introduced to PBMC cell culture via infected THP-1 macrophages, cause the relative amounts of CD3+ and CD3- lymphocytes to vary significantly. What this means for an i*n vivo* model is unknown, however, the PrfA* mutation causes *L. monocytogenes* immunogens to be overexpressed. It can be hypothesized that these proteins can cause proliferation of CD3+ lymphocytes in lieu of CD3- lymphocytes.

IL-22 is an important cytokine involved in the adaptive and innate immune response (Pestka *et. al.* 2004). Understanding the role of IL-22 with respect to T cell kinetics is of importance in the field of cellular immunity. The use of *Listeria monocytogenes* as a vaccine vector has garnered significant attention because this organism can be easily attenuated and still manages to deliver antigenic peptides intracellularly (Yan, *et. al.* 2008). Although we could not establish a role for IL-22 in the experiment as currently designed, further investigations may allow us determine a role for IL-22 in the course of *L. monocytogenes* infection. One drawback to the current design is that the amount of IL-22 produced

may be insufficient to drive proliferation of T cells. As *L. monocytogenes* is confined to THP-1 macrophages, IL-22 may not be exported properly to the extracellular environment. Rather, IL-22 is exported into the cytoplasm of the infected macrophage, wherein the host cell's machinery processes the cytokine in proteasomes and lysosomes, destroying the cytokine. Furthermore, it is not currently known what concentration of IL-22 is sufficient to induce T cell expansion or anergy and the amount of IL-22 produced by the *Listeria* vector was not quantified. Finally, previous studies have shown that IL-22 must be attached to its cognate receptor on the cell surface of the presenting cell in order to mediate its effects on the immune system (Zeng, *et. al.* 2011). Additional investigations will be necessary to determine whether IL-22 is actually being transported to the surface to interaction with its cognate receptor.

In conclusion, this study has demonstrated a reliable method of MHC-II construction that produces relatively large amounts of MHC-II tetramer in a predictable manner. Ostensibly, the protocol can be adapted to construct any allele of MHC-II, not simply DR*201. Furthermore, we implemented a protocol that may lead to detecting superantigens in complex samples. Although more work has to be conducted on the precise culture conditions, we are confident that these short-comings can be overcome. We have also demonstrated the use of *L. monocytogenes* as a vehicle vector to deliver proteins to cells of interest. Other members in our group are using this methodology to immunize macaques against HIV, malaria and *M. tuberculosis* derived proteins. Although this study did not conclusively assign a role to IL-22, some interesting data was nevertheless produced. The revelation that CD3- cells are underrepresented in prfA* infected cells was not expected and warrants

further investigation as to the precise mechanism of activation. This could lead to a better understanding of *L. monocytogenes* based vaccine vectors, either by prfA* mutants or IL-22-based therapies.

Cited Literature

Butcher, E., Williams, M., Youngman, K., Rott, L., Briskin, M. 1999. Lymphocyte trafficking and regional immunity. *Adv Immunol*. 72:209-53.

Brandes, M., Willimann, K., Moser, B. 2005. Professional antigen-presentation function by human gammadelta T Cells. *Science*. 8:309(5732):264-8.

Chan, J., Fan, X., Hunter, S., Brennan, J., and Bloom, B. 1991. Lipoarabinomannan, a possible virulence factor involved in persistence of Mycobacterium tuberculosis within macrophages. *Infect Immun*. 59(5): 1755–1761.

Cole D., Pumphrey N., Boulter J., Sami M., Bell J., Gostick E., Price D., Gao G., Sewell A., Jakobsen B. 2007. Human TCR-binding affinity is governed by MHC class restriction. *J. Immunol*. 1:178(9):5727-34.

De Luca, A., Zelante, T., D'Angelo, C., Zagarella, S., Fallarino, F., Spreca, A., Iannitti, R., Bonifazi, P., Renauld, J., Bistoni, F., Puccetti, P., Romani, L. 2010. IL-22 defines a novel immune pathway of antifungal resistance. *Mucosal Immunol*. 3(4):361-73.

Dubin, P., Kolls, J. 2008. Th17 cytokines and mucosal immunity. *Immunol Rev*. 226:160-71.

Eckburg, P., Bik, E., Bernstein, C., Purdom, E., Dethlefsen, L., Sargent, M., Gill, S., Nelson, K., Relman, D. 2005. Diversity of the human intestinal microbial flora. *Science*. 10:308(5728):1635-8.

Hanahan, D. 1983. Studies on transformation of Escherichia coli with plasmids. *J. Mol. Biol.* 166:557–580.

Hendrickson, W. 1989. Crystal Structure of Core Streptavidin Determined from Multiwavelength Anomalous Diffraction of Synchrotron Radiation. *Proceedings of the National Academy of Sciences.* 86(7): 2190–4.

Hong W., Zhimei F., and Morita, C. 2011. Vγ2Vδ2 T Cell Receptor Recognition of Prenyl Pyrophosphates Is Dependent on All CDRs. *The Journal of Immunology.* 184:6209–6222.

Kaufmann, S. 1993. Immunity to intracellular bacteria. *Annu Rev Immunol*. 11:129-63.

Kostelny, S., Link, B., Tso, Y., Vasquez, M., Jorgensen, B., Wang, H., Hall, W., & Weiner, G. 2001. Humanization and Characterization of the anti-HLA-DR antibody 1D10. *Int. J. Cancer.* 93:556-565.

Laemmli, U. 1970. Cleavage of structural proteins during the assembly of the head of bacteriophage T4. Nature 227, 680-685.

Llewelyn, M., Cohen, J. 2002. Superantigens: microbial agents that corrupt immunity. *Lancet Infectious Diseases.* Volume: 2 Issue: 3 Pages: 156-162.

Manganelli, R., Voskuil, M., Schoolnik, G., Smith, I. 2001. The Mycobacterium tuberculosis ECF sigma factor sigmaE: role in global gene expression and survival in macrophages. *Mol Microbiol*. 41(2):423-37.

Massey, R., Scriba, T., Brown, E., Phillips, R., Sewell, A. 2007. Use of peptide-major histocompatibility complex tetramer technology to study interactions between *Staphylococcus aureus* proteins and human cells. *Infect Immun*. 75(12):5711-5.

Melichar, B., Nash, M., Lenzi, R., Platsoucas, C., Freedman, R. 2000. Expression of costimulatory molecules CD80 and CD86 and their receptors CD28, CTLA-4 on malignant ascites CD3+ tumour-infiltrating lymphocytes (TIL) from patients with ovarian and other types of peritoneal carcinomatosis. *Clin Exp Immunol*. 119(1):19-27.

Xie, M., Aggarwal, S., Ho, W., Foster, J., Zhang, Z., Stinson, J., Wood, W., Goddard, A., and Gurney, A. 2000. Interleukin (IL)-22, a Novel Human Cytokine That Signals through the Interferon Receptor-related Proteins CRF2–4 and IL-22R. *J. Biol. Chem*. 275:31335-31339.

Neutra, M., Kozlowski, P. 2006. Mucosal vaccines: the promise and the challenge. *Nat Rev Immunol*. 6(2):148-58.

Nigou, J., Zelle-Rieser, C., Gilleron, M., Thurnher, M., Puzo, G. 2001. Mannosylated lipoarabinomannans inhibit IL-12 production by human dendritic cells: evidence for a negative signal delivered through the mannose receptor. *J Immunol*. 15:166(12):7477-85.

Novick, R. 2003. Autoinduction and signal transduction in the regulation of staphylococcal virulence. *Molecular Microbiology.* 48(6): 1429-1449.

Pestka, S., Krause, C., Sarkar, D., Walter, M., Shi, Y., Fisher, P. 2004. Interleukin-10 and related cytokines and receptors. *Annu. Rev. Immunol*. 22: 929–79.

Reed, M., Domenech, P., Manca, C., Su, H., Barczak, A., Kreiswirth, B., Kaplan, G., Barry, C. 2004. A glycolipid of hypervirulent tuberculosis strains that inhibits the innate immune response. *Nature*. 431(7004):84-7.

Renzoni A., Klarsfeld A., Dramsi S., Cossart P. 1997. Evidence that PrfA, the pleiotropic activator of virulence genes in Listeria monocytogenes, can be present but inactive. *Infect Immun*. 65(4): 1515–1518.

Sanos, S., Vonarbourg, C., Mortha, A., Diefenbach, A. 2011. Control of epithelial cell function by interleukin-22-producing RORγt+ innate lymphoid cells. *Immunology*. 132(4):453-65.

Schlievart, P., Case, L., Strandberg, K., Abrams, D., and Leung, D. 2008. Superantigen Profile of *Staphylococcus aureus Isolates* from Patients with Steroid-Resistant Atopic Dermatitis. *Clin Infect Dis*. 46(10): 1562-1567.

Smith, I. 2003. Mycobacterium tuberculosis pathogenesis and molecular determinants of virulence. *Clin Microbiol Rev*. 16(3):463-96.

Starks, H., Bruhn, K., Shen, H., Barry, R., Dubensky, T., Brockstedt, D., Hinrichs, D., Higgins, D., Miller, J., Giedlin, M., Bouwer, H. 2004. Listeria monocytogenes as a vaccine vector: virulence attenuation or existing antivector immunity does not diminish therapeutic efficacy. *J Immunol*. 1:173(1):420-7.

Trickett, A., Kwan, Y. 2003. T cell stimulation and expansion using anti-CD3/CD28 beads. *Journal of Immunological Methods.* 275(1-2):251-255.

Qin, G., Mao, H., Zheng, J., Sia, S., Liu, Y., Chan, P., Lam, K., Peiris, J., Lau, Y., Tu, W. 2009. Phosphoantigen-expanded human gammadelta T cells display potent cytotoxicity against monocyte-derived macrophages infected with human and avian influenza viruses. *J Infect Dis.* 15:200(6):858-65.

Villadangos, J., Schnorrer, P., Wilson, N. 2005. Control of MHC class II antigen presentation in dendritic cells: a balance between creative and destructive forces. *Immunol Rev*. 207:191-205.

Watanabe-Ohnishi, R., Low D., McGeer A., Stevens D., Schlievert P., Newton D., Schwartz B., Kreiswirth B., Kotb M. 1995. Selective depletion of V beta-bearing T cells in patients with severe invasive group A streptococcal infections and streptococcal toxic shock syndrome. *The Journal of infectious diseases.* 171(1):74-84.

Wei, H., Wang, R., Yuan, Z., Chen, C., Huang, D. 2009. DR*W201/P65 Tetramer Visualization of Epitope-Specific CD4 T-Cell during *M. tuberculosis* Infection and Its Resting Memory Pool after BCG Vaccination. *PLoS ONE* 4(9).

Wooldridge, L., Lissina, A., Cole, D., van den Berg, H., Price, D., Sewell, A. 2009. Tricks with tetramers: how to get the most from multimeric peptide-MHC. *Immunology*. 126(2):147-64.

World Health Organization. 2009. Epidemiology. Global tuberculosis control: epidemiology, strategy, financing.

Xavier, R., Podolsky, D. 2007. Unravelling the pathogenesis of inflammatory bowel disease. *Nature*. 26;448(7152):427-34.

Yan, L., Qiu, J., Chen, J., Ryan-Payseur, B., Huang, D., Wang, Y., Rong, L., Melton-Witt, J., Freitag, N., Chen, Z. 2008. Selected prfA* Mutations in Recombinant Attenuated Listeria monocytogenes Strains Augment Expression of Foreign Immunogens and Enhance Vaccine-Elicited Humoral and Cellular Immune Responses. *Infect Immun*. 76(8): 3439–3450.

Yao, S., Huang, D., Chen, C., Halliday, L., Zeng, G., Wang, R., Chen, Z. 2010. Differentiation, distribution and gammadelta T cell-driven regulation of IL-22-producing T cells in tuberculosis. *PLoS Pathog*. 26;6(2).

VITA

NAME: Omar Hassan Jawaid

EDUCATION: B.S. Biology, Loyola University Chicago, Chicago, Illinois 2005.

B.S. Psychology, Loyola University Chicago, Chicago, Illinois 2005.

M.S. Microbiology/Immunology, University of Illinois Chicago, Chicago, Illinois 2012.

TEACHING: Department of Biology, Loyola University Chicago.
Introduction to Biology 101 and 102.

HONORS: Graduated Cum Sum Laude with honors in Biology and Psychology from Loyola University Chicago, 2005.